THE ROLE OF THE ALVEOLAR MACROPHAGE IN CARBON NANOTUBE ELICITED MURINE MODEL OF PULMONARY GRANULOMATOUS INFLAMMATION

By

Matthew Kyle McPeek

September, 2018

Director of Dissertation: Mary Jane Thomassen, Ph.D.

Major Department: Interdisciplinary Program in Biological Sciences

Pulmonary sarcoidosis is a debilitating inflammatory condition characterized by the presence of granulomatous lesions throughout the lung. Granulomas are a physiological response to inhaled antigens or particulate matter which cannot be properly degraded. To explore mechanisms of granuloma formation and maintenance our laboratory developed a murine model of pulmonary granulomatous inflammation elicited by multi-wall carbon nanotubes (MWCNT). We have found the MWCNT model bears striking similarities to pulmonary sarcoidosis pathophysiology, including increased expression of inflammatory mediators and decreased expression and activity of peroxisome proliferator activated receptor-γ (PPARγ) in alveolar macrophages. PPARγ is a known regulator of macrophage activation and serves a crucial role in pulmonary

lipid homeostasis through the regulation of macrophage ATP-binding cassette (ABC) lipid transporter-G1 (ABCG1). Further studies demonstrated that alveolar macrophages obtained from sarcoidosis patients and MWCNT instilled animals have decreased gene expression and protein levels of ABCG1 and ABCA1, a complementary cholesterol transporter. These studies aim to further define the role of alveolar macrophage PPARγ, ABCA1 and ABCG1 in pulmonary granulomatous inflammation. We hypothesized that deficiency of ABCA1 and ABCG1 would exacerbate MWCNT induced granuloma formation. To test this hypothesis, macrophage-specific ABCA1, ABCG1 or combined ABCA1/ABCG1 knockout mice were developed and evaluated following MWCNT instillation. We found that deficiency of ABCG1 but not ABCA1 leads to a significant upregulation of pro-inflammatory mediators and promotes pulmonary granuloma formation. Interestingly, the combined deficiency of ABCA1/ABCG1 leads to an exacerbated pulmonary inflammatory phenotype. We further hypothesized that upregulation of the PPARγ-ABCG1 pathway would limit MWCNT induced granuloma formation and inflammation. To test this hypothesis, we administered the PPARγ-specific ligand rosiglitazone to MWCNT instilled animals and evaluated the effect on granulomatous inflammation. We found that the administration of rosiglitazone promotes the expression of alveolar macrophage ABCG1, limits the severity of MWCNT induced granuloma formation and reduced alveolar macrophage pro-inflammatory gene expression. These studies suggest that the PPARγ-ABCG1 pathway, specifically the deficiency of alveolar macrophage ABCG1 plays a significant role in pulmonary granulomatous inflammation.

THE ROLE OF THE ALVEOLAR MACROPHAGE IN CARBON NANOTUBE ELICITED MURINE MODEL OF PULMONARY GRANULOMATOUS INFLAMMATION

A Dissertation

Presented to the Faculty of the Department of Internal Medicine

Brody School of Medicine, East Carolina University

In Partial Fulfillment of the Requirements for the Degree

Doctor of Philosophy in Interdisciplinary Biological Sciences

By

Matthew Kyle McPeek

September, 2018

THE ROLE OF THE ALVEOLAR MACROPHAGE IN CARBON NANOTUBE ELICITED MURINE MODEL OF PULMONARY GRANULOMATOUS INFLAMMATION

by

Matthew Kyle McPeek

APPROVED BY:

DIRECTOR OF DISSERTATION: _____
Mary Jane Thomassen, Ph.D.

COMMITTEE MEMBER: _____
Kymberly Gowdy, Ph.D.

COMMITTEE MEMBER: _____
Kvin Lertpiriyapong, DVM, Ph.D.

COMMITTEE MEMBER: _____
Arjun Mohan, MD

COMMITTEE MEMBER: _____
Christopher Wingard, Ph.D., MS

COMMITTEE MEMBER: _____
Debra Ann Tokarz, DVM, Ph.D.

DIRECTOR OF PROGRAM: _____
Li Yang, Ph.D.

DEAN OF THE GRADUATE SCHOOL: _____
Paul J. Gemperline, Ph.D.

TABLE OF CONTENTS

LIST OF TABLES

CHAPTER TWO

LIST OF FIGURES

CHAPTER TWO

CHAPTER THREE

CHAPTER FOUR

LIST OF ABBREVIATIONS

ABCA1:	ATP-binding cassette lipid transporter A1
ABCG1:	ATP-binding cassette
apoA1:	Apoliporotein-A1
BAL:	Bronchoalveolar lavage
CCL2:	(C-C motif) ligand 2
CD36:	Cluster of differentiation - 36
cDNA:	Complementary deoxyribonucleic acid
CNT:	Carbon nanotubes
CT:	Cycle threshold
DNA:	Deoxyribonucleic acid
GAPDH:	Glyceraldehyde 3 phosphate dehydrogenase
HDL:	High Density Lipoprotein
HMGCR:	3-Hydroxy-3-Methylglutaryl-CoA Reductase
Kg:	Kilogram
KO:	Knockout
LDL-R:	Low density lipoprotein receptor
LPS:	Lipopolysaccharide
mL:	Milliliter
mm^3:	Cubic millimeter
mRNA:	Messenger ribonucleic acid
MWCNT:	Multi-wall carbon nanotubes
ng:	Nano-gram
NF-KB:	Nuclear factor kappa-light-chain-enhancer of activated B cells

PBS:	Phosphate buffered saline
PDGFα:	Platelet Derived Growth Factor Subunit A
pg:	Pico-gram
PPAR:	Peroxisome proliferator-activated receptor
PPARγ- KO:	Peroxisome proliferator-activated receptor-gamma knockout
PPRE:	Peroxisome proliferator-activated receptor response element
RNA:	Ribonucleic acid
RPM:	Revolutions per minute
RT-PCR:	Real time-polymerase chain reaction
SEM:	Standard error of the mean
TGFβ:	Transforming growth factor-beta
TLR:	Toll-like receptor
TNFα:	Tumor necrosis factor-alpha
μg:	microgram
μL:	microliter

CHAPTER ONE

INTRODUCTION

Sarcoidosis:

Sarcoidosis is an enigmatic multisystem inflammatory disorder characterized by the presence of non-necrotizing granulomas. While any organ can be affected, lung involvement has been reported in more than 90% of clinical cases [23]. Diagnosis is dependent on excluding the presence of an infectious agent or a prior exposure to a material known to produce granulomatous lesions [137]. The clinical stages of pulmonary sarcoidosis are defined as hilar lymph node involvement (Stage I), granulomatous infiltrates into the parenchyma of the lung (Stage II), bilateral infiltrates without lymph node involvement (Stage III) and progressive pulmonary fibrosis (Stage IV) [137]. However, the clinical manifestation of the disease is variable, spontaneous remission has been reported in two thirds of individuals whereas progression is associated with significant morbidity and mortality [72;84]. The most common cause of sarcoidosis related death is respiratory failure, particularly among older individuals [24;72;129]. Recent studies also indicate that the incidence of sarcoidosis and related hospitalization has increased during the past few decades [43;46].

Despite extensive research, the etiology of this disease remain unclear. The prevalence of sarcoidosis varies around the world. High rates of sarcoidosis have been reported in Finland (28.2:100,000), while the incidence in Japan (3.7:100,000) is one of the lowest in the world [110]. In the United States, the incidence among African Americans (39:100,000) is 12 times higher than Caucasians (5:100,000) and this demographic has an increased rate of associated morbidity and mortality [67;94;120]. These observations suggested genetic predisposition may play a role in the pathophysiology of sarcoidosis. Bioinformatic studies have implicated changes in

specific human leukocyte antigen (HLA) genes which may influence susceptibility to the sarcoidosis, however, these changes varied between patient populations [20;32;119]. Similar inconsistencies have been found with non-HLA candidate genes identified through genome-wide search approaches [123]. These observations suggest that other environmental factors influence the pathogenesis of sarcoidosis.

Due to the histological and clinical similarities between pulmonary sarcoidosis and mycobacterium infections, the involvement of infectious agents have been investigated. Utilizing polymerase chain reaction and mass spectrometry approaches, the presence of mycobacterial DNA and protein fragments have been identified in sarcoidosis lesions [52;105]. Further evidence which supports a role for a specific eliciting antigen is the Kveim reaction. First observed by Ansger Kveim in 1941, intradermal injection of sarcoidosis tissue homogenate produces histologically similar granulomas within several weeks [77]. Further studies conducted in the 1960's found that 50-80% of sarcoidosis patients have a positive Kveim reaction [124]. Despite these observations, extensive studies have been performed to identify the presence of an active microorganism in clinical biopsy samples with no success [29;93]. These finding may suggest a role for microbial agents during the onset of sarcoidosis but, given the heterogeneity of the disease, there is likely more than one etiology.

While the lungs and associated lymph nodes are the most commonly affected organ, cutaneous and ocular sarcoidosis are also reported in 25% of clinical cases [62]. A common feature of these organs is the continuous exposure to the external environment where particulate matter may play a role in propagation of the disease. To identify potential environmental risk factors, the ACCESS (A Case Control Etiologic

Study of Sarcoidosis) study was conducted. Although a single causative antigen was not identified, a previous exposure to moldy environments, insecticides, industrial organic dust or metal particulates were associated with the development of sarcoidosis [75;101]. Other reports found the incidence of sarcoidosis to be most prevalent in rural areas [67]. Assessment of potential risk factors included the use of wood stoves and fireplaces [68]. These observations indicate that air-borne particulate matter may play a significant role in the disease.

Further research will be required to determine how genetics, infectious agents and the environment contribute to the pathobiology of sarcoidosis. Currently, our understanding suggest the development of sarcoidosis results from an exuberant host immune response to a poorly soluble antigen in genetically susceptible individuals [25;97;101]. Macrophages are the primary immune cell tasked with the removal of foreign antigens. Understanding how these cells contribute to the formation of granulomas may lead to improved therapies for granulomatous diseases.

Macrophages:

Macrophages are terminally differentiated monocytes named for the tissue in which they reside. Since the original description by Metchnikoff, the macrophage has been recognized as the professional phagocyte of the immune system [99]. Alveolar macrophages are the predominant cell type found in the lower airways of healthy individuals and play an integral role in maintaining pulmonary homeostasis [41;125]. The unique environment of the lung plays a key role in shaping the phenotype of the alveolar macrophage [61]. The lower airways are coated in a lipid rich film, called surfactant, and are constantly exposed to the external environment. The alveolar

macrophage plays a role in both the regulation of surfactant catabolism and the clearance of inhaled particulate matter. The inability to efficiently clear surfactant or properly degrade inhaled antigens can result in significant pulmonary inflammation.

Alveolar Macrophages and Lipid Homeostasis:

Pulmonary surfactant is a complex mixture of approximately 90% lipids and 10% proteins [53]. Synthesized and secreted by alveolar type 2 cells, surfactant acts to lower the surface tension of the alveoli which prevents their collapse. Surfactant turnover is equally important to pulmonary homeostasis. Surfactant can be endocytosed and recycled by alveolar type 2 cells or catabolized by alveolar macrophages [140;141]. Catabolized lipids are removed from the macrophage by reverse cholesterol transport pathways specifically the transcription factor peroxisome proliferator activated receptor gamma (PPARγ) and its downstream target ATP binding cassette lipid transporter-G1 (ABCG1). Deficiency of this pathway results in significant pulmonary lipid accumulation and pro-inflammatory inflammation [131].

Peroxisome Proliferator Activated Receptor - γ:

PPARγ is a ligand activated nuclear transcription factor which promotes lipid and glucose metabolism and negatively regulates macrophage activation by antagonizing the activity of pro-inflammatory mediators [49;132]. Evaluation of alveolar macrophages isolated from healthy individuals found constitutively high expression and nuclear localization of PPARγ [27]. The deficiency of PPARγ has been reported in several lung diseases including pulmonary hypertension, allergic airway inflammation, and

sarcoidosis [4;27;35;73]. The unique lipid rich environment of the lung coupled with the constant exposure to the environment suggest that alveolar macrophage PPARγ may play a unique role in pulmonary homeostasis.

To further investigate alveolar macrophage PPARγ, macrophage-specific PPARγ knockout mice (PPARγ-KO) have been characterized. PPARγ-KO animals demonstrate significant lipid accumulation in alveolar macrophages and the lower airways [7]. Further studies found PPARγ-KO alveolar macrophages were deficient in the lipid transporter ABCG1 [7]. The expression of the complimentary lipid transporter ABCA1 is upregulated in these animals, likely compensating for the deficiency of ABCG1 [7;45;134]. In addition to pulmonary lipid accumulation, PPARγ-KO animals exhibit a pro-inflammatory pulmonary phenotype, characterized by elevated expression of interferon-γ and inducible nitric oxide synthase [88]. Restoration of PPARγ via lenti-viral transduction significantly attenuated both pulmonary lipid accumulation and pulmonary inflammation [6;88]. These observations suggest that alveolar macrophage PPARγ plays an integral role maintaining pulmonary homeostasis.

ATP-Binding Cassette Lipid Transporters:

The lipid transporters ABCA1 and ABCG1 play an important role in the export of catabolized lipids from the cell. Following phagocytosis, surfactant lipids are catabolized and effluxed to the extracellular acceptors apolipoprotein-A1 and high density lipoprotein, by ABCA1 and ABCG1 respectively [80;135]. In addition to reverse cholesterol transport, ABCA1 and ABCG1 play an important role in innate immune signaling pathways. Deficiency of either of these lipid transporters leads to macrophage

lipid accumulation and increased production of inflammatory mediators [70;106;146]. Evaluation of ABCA1 or ABCG1 knockout mice found macrophages from these animals have increased formation of lipid rafts, cholesterol rich membrane microdomains which organize cell signaling molecules such as toll like receptors [74;147]. Accumulating evidence has found that dyslipidemia, particularly dysregulation of macrophage reverse cholesterol transport pathways, can greatly influence innate immunity and promote pulmonary inflammation. Interestingly, lipid loaded macrophages have been observed in several lung diseases including pneumonia and pulmonary fibrosis [17].

Alveolar Macrophages and Inhaled Particulate Matter:

In addition to surfactant catabolism, alveolar macrophages are also tasked with the clearance of particulate matter and other foreign antigens from the lower airways. The majority of inhaled particulate matter is arrested as it passes over the mucosal lining of the nasal cavity and bronchial tree, only a fraction reaches the lower airways where gas exchange is paramount. An overt inflammatory response to each inhaled inert particulate would significantly impede gas exchange. Interestingly, studies have found alveolar macrophages have a reduced capacity to elicit immune responses and limit the release of pro-inflammatory mediators following stimulus [55;81;85]. These observations suggest alveolar macrophages act to limit pulmonary inflammation. Alveolar macrophages likely play a role in the progression of sarcoidosis by retaining the eliciting antigen and propagating pulmonary granuloma formation. Intradermal injection of bronchoalveolar lavage (BAL) cell homogenate, which consisted predominately of macrophages, was found to elicit granulomatous inflammation similar

to the Kveim reagent [56]. Furthermore, as in other tissues of the body, the inability of the macrophage to properly degrade a foreign antigen results in the formation of a granuloma [64].

Granuloma:

The granuloma is a physiologic response to a foreign antigens which cannot be broken down by the mononuclear phagocyte system, intended to protect the surrounding tissue from further damage [107]. When an antigen is phagocytosed, the macrophage releases chemoattractants which recruit other immune cells to assist in the clearance of the substance. If the macrophages are unable to clear the material, a milieu of cytokines and chemokines are released which promote the fusion and transformation of macrophages into an epithelioid granuloma [3;102]. Sarcoidosis granulomas are non-necrotizing, indicating the absence of a necrotic core which is observed in other infectious granuloma where the eliciting agent can survive. The granuloma consist of epithelioid macrophages, fibroblast with occasional CD4+/CD8+ T-cells associated with the periphery of the structure [1]. The presence of the granuloma in the lung can cause significant airway obstruction and as observed in progressive sarcoidosis, if unresolved can be replaced with collagen and other matrix proteins resulting in tissue fibrosis.

Granulomatous Lung Disease:

Granulomatous lung disease represents a significant health burden worldwide. However, investigating the mechanisms of pulmonary granuloma formation have been impeded by the lack of viable animal models. Previous models have utilized various methods to induce granulomas, including the administration of pathogens or introduction of antigen bound sepharose beads injected into the tail vein of sensitized animals [33;63;76]. While these models advanced the understanding of granuloma formation they have suffered significant drawbacks including the presence of an active pathogens, eliciting granuloma formation from the pulmonary capillaries instead of the airways and relatively short resolution time, between 14 and 21 days. Characteristics which are not observed in pulmonary sarcoidosis. To investigate underlying mechanisms of chronic granuloma formation our laboratory investigated the use of carbon nanomaterials.

Carbon Nanomaterials:

Carbon nanomaterial are produced for use in industrial processes or as the byproducts of combustion. The interest in nanotechnology and its wide range of commercial applications began in 1985 with the generation of the “buckyball,” a spherical arrangement of carbon atoms which earned the 1996 Nobel Prize in Chemistry [78]. Further efforts led to the generation of elongated, cylindrical arrangements of carbon atoms referred to as carbon nanotubes (CNT) which can be generated as a single wall carbon nanotube (SWCNT) or, with the addition of consecutive layers of carbon, multiwall carbon nanotubes (MWCNT). These materials

have been shown to have incredibly unique characteristics. Nanotubes are predicted to be stronger than steel and may conduct electricity better than copper [37]. Outside of manufacturing processes, MWCNT can also be found ubiquitously within our environment. Particulate matter collected from the urban centers of El Paso and Houston Texas contained MWCNT, likely the byproducts of vehicle exhaust [98]. Indoor environments also harbor MWCNT of respirable sizes. Samples collected from propane or natural gas flames, including those of typical stoves and heaters, contained particulates consisting of nearly pure carbon nanoparticles [12].

Nanomaterials and Respiratory Health:

As the potential applications and production capacity of these materials increased, environmental exposure has become a concern. The first study to evaluate the pulmonary toxicity of carbon nanotubes was conducted by Lam et al. in 2004. The authors found that intratracheal instillation of SWCNT induced dose dependent epithelioid granulomatous lesions in the lungs of mice at 7 and 90 days post instillation [79]. Studies utilizing MWCNT showed a similar pulmonary responses in Sprague-Dawley rats 60 days post intratracheal instillation [96]. It was also determined that particle size influenced the toxicity of both types of CNT, ultrasonification or physical disruption increased the distribution and severity of granulomatous lesions [79;96]. These observations suggested that particulate matter of respirable sizes, particularly carbon nanomaterials, can adversely impact human health [37;78]. Interestingly, granulomatous lesions have been reported in the lungs of firefighters and non-

firefighting individuals present at the site of the September 2001 World Trade Center (WTC) disaster [34;65;92]. Further analysis of WTC dust and lung tissue from exposed individuals found the presence of carbon nanotubes.

MWCNT Induced Model of Chronic Granuloma Formation:

The observation that carbon nanotubes have the capacity to induce granulomatous lesions prompted Huizar et al. to investigate the use of purified MWCNT to generate a murine model of chronic granuloma formation. Following oropharyngeal instillation, pulmonary granulomas were first evident 10 days following instillation and persisted 90 days after exposure [58]. Characterization of the lesions found the presence of macrophages and CD3+ T-cells, characteristics of well-formed granulomas [58]. Further evaluation of granulomatous tissue collected by microdissection found increased expression of cellular adhesion molecules and matrix-remodeling proteins which had been reported in pulmonary sarcoidosis patients [58]. These observations suggest the MWCNT model could be used to investigate cellular and molecular mechanisms which contribute to the persistence of pulmonary granulomas.

Our laboratory has previously demonstrated alveolar macrophages of healthy individuals exhibit constitutively high expression and activity of PPARγ [27], a nuclear transcription factor and negative regulator of pro-inflammatory macrophage activation [116]. In contrast, alveolar macrophages isolated from sarcoidosis patients are deficient of PPARγ gene expression and DNA binding activity [35]. Evaluation of alveolar macrophages following MWCNT instillation found reduced PPARγ mRNA expression

and nuclear localization compared to sham instilled mice [59]. This observation suggest PPARγ pathways may play a role in pulmonary granuloma formation.

PPARγ Deficiency Exacerbates MWCNT Induced Granulomatous Inflammation:

To further evaluate the role of alveolar macrophage PPARγ, macrophage-specific PPARγ knockout mice (PPARγ-KO) were utilized. Sixty days following MWCNT instillation, PPARγ-KO animals were found to develop increased frequency and severity of pulmonary granulomas [59]. The expression of chemokine (C-C motif) ligand 2 (CCL2) and osteopontin were also evaluated in wild-type and PPARγ-KO animals following MWCNT instillation. Murine studies have found deficiency of CCL2 or osteopontin limits pulmonary granuloma formation [83;104]. The expression of CCL2 and osteopontin are intrinsically elevated in PPARγ-KO alveolar macrophages compared to wild-type animals [59]. Following MWCNT instillation, the expression of CCL2 and osteopontin was significantly increased in wild-type animals and further elevated in PPARγ-KO bearing nanotubes [59]. [58;59]. These data suggest the expression of CCL2 and osteopontin correlate with the severity of pulmonary granuloma formation.

PPARγ Pathways are Dysregulated in MWCNT Model:

To further evaluate the effect of MWCNT induced PPARγ deficiency, PPARγ regulated genes were evaluated. Previous studies have demonstrated alveolar macrophage PPARγ promotes the expression of the lipid transporter ABCG1, and limits alveolar macrophage lipid accumulation [6]. Evaluation of BAL cells from MWCNT

instilled animals found a significant decrease in both the expression and protein levels of ABCG1 and ABCA1 [16]. The deficiency of these lipid transporters also correlated with an increase of intracellular lipid accumulation in MWCNT instilled mice [16], a phenotype shown to promote pro-inflammatory macrophage activation [147]. These observations suggest that the deficiency of ABCA1 and ABCG1 may promote alveolar macrophage pro-inflammatory activation following the instillation of MWCNT.

General Hypothesis:

Our previous studies have shown the MWCNT model bears striking similarity to pulmonary sarcoidosis, including the deficiency of alveolar macrophage PPARγ and the PPARγ-regulated cholesterol transporter ABCG1 [16;35;59]. Based on these observations, we hypothesized that deficiency of the PPARγ-ABCG1 pathway and increased pulmonary lipid accumulation would promote MWCNT induced granulomatous inflammation. To address this hypothesis, macrophage specific ABCA1, ABCG1 or combined ABCA1/ABCG1 knockout mice were generated and evaluated for MWCNT induced granuloma formation and inflammation. To further confirm involvement of the PPARγ-ABCG1 pathway, we administered the PPARγ specific agonist rosiglitazone to MWCNT instilled animals. We hypothesized that administration of rosiglitazone would promote alveolar macrophage ABCG1 expression, limit carbon nanotube induced granuloma formation and pro-inflammatory inflammation.

CHAPTER TWO

GENERATION OF MACROPHAGE SPECIFIC ATP-BINDING CASSETTE LIPID TRANSPORTER DEFICIENT MICE

ABSTRACT

Pulmonary sarcoidosis is a chronic inflammatory condition characterized by granulomatous inflammation. We have developed a murine model of chronic granulomatous inflammation elicited by carbon nanotubes. Evaluation of alveolar macrophages from sarcoidosis patients or animals instilled with carbon nanotubes found decreased expression and protein content of the ATP-binding cassette lipid transporters ABCA1 and ABCG1. Previous studies have demonstrated that the deficiency of these genes in complete murine knockouts promotes pulmonary lipid accumulation and inflammation. To further evaluate the role of alveolar macrophage ABCA1 and ABCG1 we generated macrophage specific ABC-transporter deficient mice using the LysMCre system. We found that the deficiency of ABCG1 and to a further extent, combined deficiency of ABCA1/ABCG1 promote pulmonary lipid accumulation and pro-inflammatory alveolar macrophage gene expression. Interestingly, ABCA1 deficiency did not affect pulmonary lipid homeostasis or inflammation. These observation suggest that alveolar macrophage ABCG1 acts as a critical regulator of pulmonary homeostasis.

INTRODUCTION

Our laboratory has described a multi-wall carbon nanotube (MWCNT) induced murine model of chronic granuloma formation [58]. We have found that this model bears striking similarity to pulmonary sarcoidosis, a disease characterized by the presence of granulomatous inflammation. We have recently demonstrated that alveolar macrophages of both sarcoidosis patients and MWCNT instilled mice have reduced gene expression and protein content of the lipid transporters ATP-binding cassette lipid transporter-A1 (ABCA1) and ABCG1 [16]. ABCA1 and ABCG1 are transmembrane proteins which facilitate the transport of lipids across plasma membranes. [39;80]. The deficiency of these lipid transporters in the MWCNT model correlate with increased alveolar macrophage lipid accumulation, a phenotype shown to induce pro-inflammatory macrophage activation [139;147].

ABCA1 and ABCG1 expression is variable throughout the body, however both are expressed in multiple cell types of the lung. The presence of ABCA1 has been found in type I and type II pneumocytes and alveolar macrophages [18;28;71]. ABCG1 is expressed in type II pneumocytes, alveolar macrophages, T-lymphocytes, dendritic cells and airway smooth muscle cells [40;70]. Alveolar macrophage ABCA1 and ABCG1 are particularly important in the catabolism of pulmonary surfactant. Produced by type II pneumocytes, surfactant reduces the surface tension of the airways and prevents alveolar collapse [140;141]. Approximately 50% of surfactant is recycled by type II pneumocytes while the remaining is catabolized by alveolar macrophages [140;141]. Following catabolism, surfactant lipids are transferred to the extracellular acceptors apolipoprotein-A1 and high-density lipoprotein by ABCA1 and ABCG1

respectively [39;80]. Deficiency of either lipid transporter has been shown to promote pulmonary lipid accumulation. ABCA1 deficient mice develop progressive pulmonary lipid accumulation which is first observed at 4-months, although not as severe as animals evaluated at 7-, 12- or 18- months of age [19;90]. Surfactant producing, type II pneumocytes of these animals also demonstrate abnormal morphology and increased cholesterol content [19]. ABCG1 deficient animals develop lipid accumulation in the periphery of the lung as early as 3 weeks of age [143]. At 8 months, ABCG1 deficient animals have stark lipid accumulation in all parts of the lung and altered morphology of type 2 pneumocytes [11;70]. The observed changes in lung morphology were exacerbated by the administration of high-fat, high-cholesterol-diet [10]. While these observations are striking, and demonstrate an important role for ABCA1 and ABCG1 in pulmonary lipid homeostasis, establishing how specific cell types contribute to the phenotype is challenging in complete knockout animals.

To determine the role of alveolar macrophage lipid transporter deficiency in granulomatous lung disease, our laboratory developed macrophage-specific knockout animals using the Cre/lox system. The Cre/*lox* system has become a powerful tool used to develop tissue specific knockout animals. Originally described by Nat Sternberg, the technique utilizes the bacteriophage DNA recombinase *Cre*, and the specific locus of crossover sequence *loxP* adapted for use in higher eukaryotes [144]. Briefly, a murine strain is developed which expresses the *Cre recombinase* protein in place of a gene found exclusively in a tissue of interest. In a separate mouse model, *loxP* sites – specific DNA sequences recognized by *Cre recombinase* – are inserted on either side of a specific gene intended to be deleted, or floxed. Following selective breeding

protocols, animals homozygous for Cre recombinase and the floxed gene are produced. During development, *Cre recombinase* is produced instead of the tissue specific gene, binds the loxP sites and excises the target gene of interest. Our studies utilized *LysMCre* knock-in mice, where the *Cre recombinase* gene has been substituted in place of *lysozyme 2*. *Lysozyme 2* is only expressed in monocytes, mature macrophages and granulocytes. Here we describe the protocols used to develop macrophage-specific ABCA1, ABCG1 or ABCA1/ABCG1 knockout animals.

MATERIAL AND METHODS

Mice: All studies were conducted in accordance with the National Institutes of Health guide for the use of laboratory animals and approved by the East Carolina University Institutional Animal Care and Use Committee**.** C57Bl/6J wild-type mice were obtained from The Jackson Laboratory (Bar Harbor, ME). Macrophage-specific ATP-binding cassette (ABC) lipid transporter knockout mice were generated by crossing *Abca1*$^{flox/flox}$*Abcg1*$^{flox/flox}$ double floxed mice (catalog#021067; Jackson Laboratory) with *LyzMCre*$^{+/+}$ mice (catalog#004781;Jackson Laboratory) to generate *LysMCre*$^{+/+}$-*Abca1*$^{flox/flox}$ (ABCA1-KO), *LysMCre*$^{+/+}$*Abcg1*$^{flox/flox}$ (ABCG1-KO) or *LysMCre*$^{+/+}$*Abca1*$^{flox/flox}$*Abcg1*$^{flox/flox}$ (ABCA1/ABCG1-DKO) animals. To confirm genotypes, tail biopsies were digested in lysis buffer (400mM NaCl, 100mM pH8.0 Tris, 5mM EDTA, 0.2% SDS, 20μg/mL RNaseA, 500μg/mL proteinase K) overnight at 55^{0}C with gentle shaking followed by phenol chloroform genomic DNA purification. Polymerase chain reaction (PCR) was further conducted using KAPA Biosystems master mix (catalog # KK5621) and specific primers for LysMCre, ABCA1 or ABCG1 provided by The Jackson Laboratory (supplementary figure 1A). Finally, each reaction mixture was separated with 2% agarose gel and photographed under ultraviolet illumination for identification of specific genotypes.

Bronchoalveolar lavage (BAL): Animals were euthanized by intraperitoneal injection of tribromoethanol. BAL was performed as previously described [88]. Briefly, the trachea was canulated and lungs were sequentially lavaged with 1mL aliquots of 0.2% lidocane solution in phosphate buffered saline totaling 5mL. Following centrifugation at 1800 RPM x 10 minutes at 4°C, supernatant was snap frozen on dry

ice as BAL fluid (BALF). BAL cells were washed twice in 4mL chilled phosphate buffered saline and snap frozen as a pellet for further analysis. Differential cell counts and mean alveolar macrophage diameter were determined from BAL cell cytospins, generated by centrifugation at 500 RPM x 5 minutes and subsequently stained with Diff Quick solution (Thermo Fisher Scientific. Waltham, MA).

Analysis of Bronchoalveolar Lavage Fluid: Cholesterol content was evaluated using the Amplex Red Cholesterol Assay kit (Thermo Fisher Scientific. Waltham, MA) according to the manufacturer's instructions in the presence of cholesterol esterase.

RNA Purification and Analysis: Total RNA was isolated using the miRNeasy Micro Kit (Qiagen. Hilden, Germany) according to manufacturer's protocol. Specific primers were obtained from Qiagen for ATP binding cassette (ABC) transporter-A1 (Abca1, PPM03952F), Abcg1 (PPM03895A), chemokine (C-C motif) ligand-2 (Ccl2, PPM03151G), Glyceraldehyde-3-phosphate-dehydrogenase (Gapdh, PPM02946E) and osteopontin (Spp1, PPM03648C). Primers for low-density lipoprotein receptor (LDL-R, Mm00440169_m1) and 3-Hydroxy-3-Methylglutaryl-CoA Reductase (HMGCR, Mm1282494_g1) were obtained from Applied Biosystems (ThermoFisher. Foster City, CA). Relative gene expression of complimentary-DNA synthesized with the RT2 First Strand Kit (Qiagen) was evaluated on the Step-One-Plus, Real Time PCR system (Thermo Fisher Scientific. Waltham, MA) in comparison to Gapdh using the $2^{-\Delta\Delta CT}$ method [82].

Statistical Analysis: All data represent the mean of at least three individual experiments ±SEM unless otherwise indicated. Statistical analysis was performed using GraphPad Prizm software (San Diego, CA). Significance was determined by two-tailed student's t-

tests (2 groups) or ANOVA (>2groups) with Bonferroni's correction. For all tests, $p<0.05$ was considered statistically significant.

RESULTS

Selective Breeding Protocols Generate ATP-Lipid Transporter Deficient Mice:

Animals purchased from The Jackson Laboratory, were paired and the offspring subsequently genotyped using polymerase chain reaction utilizing the primer sets listed in Table 1. LysMCre wild-type and mutant reactions (Figure 1 A-B) were carried out independently due to non-specific primer binding. Representative images of agarose gels demonstrating homozygous wild-type (WT), heterozygous (HET) and homozygous mutant (MT) alleles for LyzMCre, ABCA1 and ABCG1 are shown in Figure 1. Animals homozygous for both LysMCre and ABCA1, ABCG1 or combined ABCA1/ABCG1 mutant alleles were used to establish colonies. Animals were subsequently genotyped for 4 generations after the establishment of the colony to ensure unintended crosses were not included in experiments.

Macrophage ABCG1 Deficiency Promotes Leukocyte Accumulation in the Lung:

To determine if macrophage deficiency of ABC-lipid transporters effects BAL cell count or composition, bronchoalveolar lavage (BAL) was performed. Previous reports have observed leukocyte infiltration in the lungs of complete ABCG1 knockouts (Wojak 2008). Following BAL, the total cell count of C57Bl/6 ($1.06x10^6 \pm 0.05$) and ABCA1-KO ($1.01x10^6 \pm 0.03$) did not statistically differ (Figure 2A). The total cell count of ABCG1-KO ($1.31x10^6 \pm 0.07$) and ABCA1/ABCG1-DKO ($1.67x10^6 \pm 0.1$) were significantly higher than wild-type animals (Figure 2A). Wojcik et al. also demonstrated increased polymorphonuclear cells (PMNs) in the lungs of ABCG1 deficient animals [143]. Evaluation of BAL cell differentials from macrophage specific knockout mice found no difference in the leukocyte composition between C57Bl/6 and ABCA1-KO mice (Figure

2B). ABCG1-KO animals had a slight but significant increase in both lymphocytes and PMNs compared to wild-type animals (Figure 2B). ABCA1/ABCG1-DKO animals demonstrate further lymphocyte and PMN infiltration compared to C57Bl/6 and ABCG1-KO animals (Figure 2B).

Lipid Regulatory Genes are Dysregulated in ABC-Lipid Transporter Deficient Macrophages:

Macrophage intracellular lipid content is regulated by the complimentary effects of uptake, synthesis and subsequent export [31]. Lipid uptake and synthesis are mediated by the low-density lipoprotein receptor (LDL-R) and 3-Hydroxy-3-Methylglutaryl-CoA (HMGCR) respectively while the export of lipids is facilitated by ABCA1 and ABCG1. Evaluation of LDL-R and HMGCR mRNA expression found a slight but non-significant decrease in ABCA1-KO, but significant downregulation in both ABCG1-KO and ABCA1/ABCG1-DKO alveolar macrophages (Figure 3). Interestingly, ABCG1 mRNA expression was significantly reduced in ABCA1-KO alveolar macrophages (Figure 3D). The expression of ABCA1 mRNA was significantly upregulated in ABCG1-KO alveolar macrophage (Figure 3C).

Macrophage Deficiency of ABCG1 Promotes Pulmonary Lipid Accumulation:

To further characterize the extent of pulmonary lipid accumulation the diameter of alveolar macrophages and cholesterol content of BAL fluid was evaluated. The mean diameter of alveolar macrophages collected from C57Bl/6 (8.5 ± 0.3μm) and ABCA1-KO (8.7 ± 0.2μm) animals did not differ in size (Figure 4A). Alveolar macrophages of ABCG1-KO (9.7 ± 0.2μm) and ABCA1/ABCG1-DKO (10.4 ± 0.1μm) were significantly

larger than those from C57Bl/6 animals, no additional increase in size was observed in double knockout mice (Figure 4A). Extracellular cholesterol content was evaluated by measuring total cholesterol and cholesterol ester of BAL fluid. Total cholesterol content of C57Bl/6 animals (1.9 ± 0.1 μg/mL) and ABCA1-KO (1.8 ± 0.1 μg/mL) did not differ (Figure 4B). ABCG1-KO (2.3 ± 0.1 μg/mL) and, to a further extent, ABCA1/ABCG1-DKO (2.9 ± 0.2 μg/mL) BAL fluid demonstrate significantly higher total cholesterol content than C57Bl/6 animals (Figure 4A). BAL fluid cholesterol ester did not differ between C57Bl/6 (0.2 ± 0.04 μg/mL) and ABCA1-KO (0.2 ± 0.03 μg/mL) but was significantly increased in ABCG1-KO (0.5 ± 0.07 μg/mL) and ABCA1/ABCG1-DKO (0.6 ± 0.04 μg/mL) animals (Figure 4C). No difference was observed between ABCG1-KO and ABCA1/ABCG1-double knockout animals.

Macrophage ABCG1 deficiency promotes pro-inflammatory gene expression:

Lipid accumulation has been shown to promote pro-inflammatory macrophage activation. We evaluated the expression of the inflammatory cytokines chemokine (C-C motif) ligand-2 (CCL2) and osteopontin in BAL cells from ABC-lipid transporter knockouts. Interestingly, the expression of CCL2 and osteopontin were significantly decreased in alveolar macrophages isolated from ABCA1-KO animals compared to C57Bl/6 mice (Figure 5). BAL cells isolated from ABCG1-KO and to a further extent ABCA1/ABCG1-DKO demonstrate significantly higher CCL2 and osteopontin expression compared to C57Bl/6 or ABCA1-KO animals (Figure 5).

DISCUSSION

Here we describe the generation of ABCA1, ABCG1 and ABCA1/ABCG1 macrophage specific knockout mice utilizing the *Cre/lox* system. We found ABCG1-KO and to a further extent ABCA1/ABCG1-DKO develop pulmonary lipid accumulation and alveolar macrophage expression of pro-inflammatory mediators. Interestingly, macrophage deficiency of ABCA1 did not affect pulmonary lipid accumulation at 8 weeks of age. These studies suggest that alveolar macrophage ABCG1 and, to a further extent, the combined deficiency of ABCA1 and ABCG1 promotes pulmonary lipid accumulation.

Previous studies have suggested the deficiency of ABCG1 acts as the primary regulator of pulmonary lipid homeostasis. Lipid deposition is observed in ABCG1 deficient mice as early as 3-weeks of age, while the earliest report in ABCA1 knockout animals is 4 months [19;143]. Wang et al. sought to quantify the contribution of macrophage ABCA1 and ABCG1 to cholesterol efflux. Those studies demonstrated that while ABCA1 deficiency reduced total cholesterol efflux, an alternative, compensatory pathway existed [136]. Further evaluation found eliminating both ABCA1 and ABCG1 further decreased total cholesterol efflux potential, demonstrating these lipid transporters cooperatively mediate cholesterol efflux [136]. Although further studies will be required, the observation that combined deficiency of ABCA1 and ABCG1 exacerbates pulmonary lipid accumulation suggest a similar mechanism takes place in the lung.

Previous studies have shown ABCG1 deficiency promotes pro-inflammatory lung inflammation. Evaluation of whole lung mRNA found increased expression of multiple

pro-inflammatory mediators including CCL2 [8]. Further evaluation of BAL fluid and alveolar macrophages from these animals found increased pro-inflammatory cytokines [143]. However, these studies did not evaluate alveolar macrophage CCL2 or osteopontin expression specifically. These observations further suggest that dysregulation of alveolar macrophage ABCG1 and pulmonary dyslipidemia effect lung homeostasis.

Table 1: Polymerase chain reaction primers utilized for the identification of ATP-binding cassette lipid transporter knockout mice.

Primer	Sequence 5’ to 3’
LyzMCre(Wild Type)	TTACAGTCGGCCAGGCTGAC
LyzMCre (Common)	CTTGGGCTGCCAGAATTTCTC
LyzMCre (Mutant)	CCCAGAAATGCCAGATTACG
Abca1 (Forward)	GATCTAGGCAGAAGGCACTTG
Abca1 (Reverse)	TTTCCCAGAGATCCCTTTCA
Abcg1 (Forward)	GTGGGGTGAGACATGTGGA
Abcg1 (Reverse)	GGAAGAAGCCTTGGGTTGA

Figure 1: Representative Image of PCR Gel Electrophoresis. Following PCR amplification, genomic DNA was separated on 2% agarose gel and photographed under ultraviolet light. Representative images of (A) LyzMCre-mutant and (B) LyzMCre wild-type, (C) ABCA1 and (D) ABCG1 PCR products. *Abbreviations: Homozygous wild-type (WT), homozygous mutant (MT) and heterozygous (HET).*

Figure 1

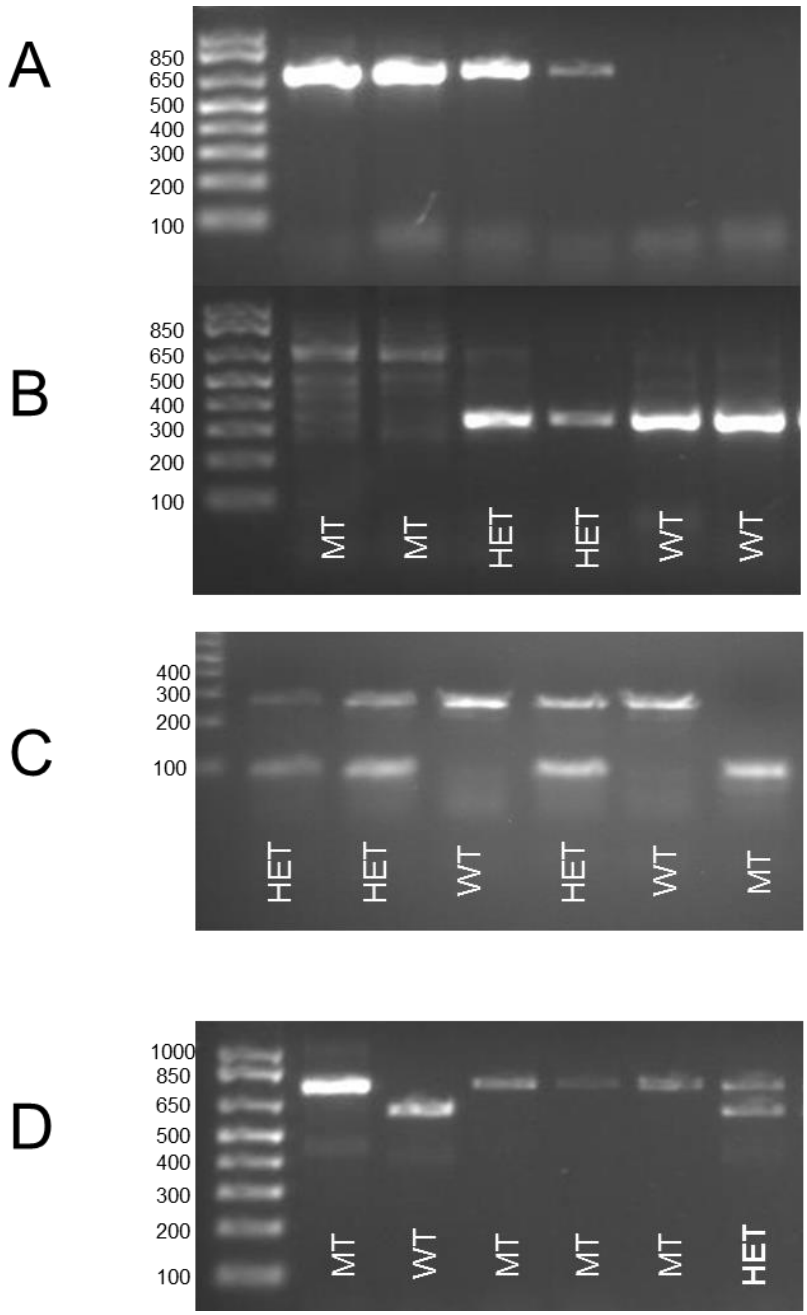
A
850
650
500
400
300
200
100
LyzMCre
Mutant Allele:700 bp
B
850
650
500
400
300
200
100
MT
MT
HET
HET
WT
WT
LyzMCre
Wild-Type Allele:350 bp
C
400
300
200
100
HET
HET
WT
HET
WT
MT
ABCA1
Wild Type Allele:277 bp
Mutant Allele: 100 bp
D
1000
850
650
500
400
300
200
100
MT
WT
MT
MT
MT
HET
ABCG1
Wild Type Allele: 600 bp
Mutant Allele: 700 bp

Figure 2: ABCG1 Deficiency Promotes Leukocyte Recruitment. (A) Total cell count and (B) leukocyte differentials of BAL cells isolated from naïve 8 week old mice. Data represent mean ± SEM n≥8, ★ $p<0.05$.

Figure 2

A

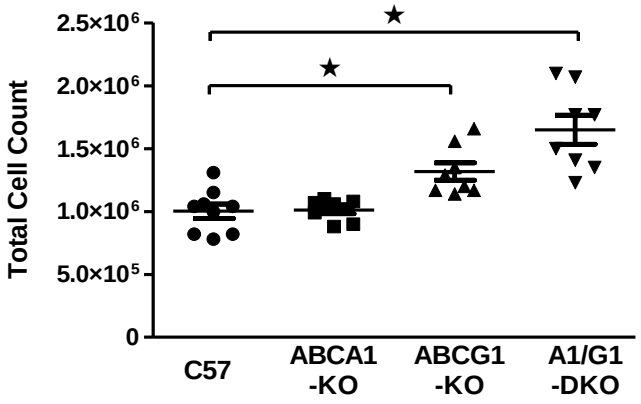

B **Leukocyte differentials of BAL cells isolated from naïve ABC-KO mice. (n≥8/strain)**

	AMs (%)	L (%)	PMN (%)
C57Bl/6J			
Mean± SEM	99.6 ± 0.3	0.2 ± 0.1	0.2 ± 0.2
ABCA1-KO			
Mean± SEM	99.7 ± 0.2	0.3 ± 0.2	0
ABCG1-KO			
Mean± SEM	94.4 ± 1.0	1.5 ± 0.3⋆	4.1 ± 1.0⋆
A1/G1-DKO			
Mean± SEM	87.6 ± 1.6	3.5 ± 0.8⋆♦	9.5 ± 2.1⋆♦

⋆ p<0.05, Knockout vs. C57Bl/6

♦ p<0.05, ABCA1/ABCG1-DKO vs ABCG1-KO

Definition of abbreviations: AMs, alveolar macrophages; L, lymphocytes; PMN, polymorphonuclear

Figure 3: Lipid Regulatory Gene Expression in ABC-knockout Mice. Quantitative-PCR analysis of (A) LDL-R and (B) HMGCR, (C) ABCA1 and (D) ABCG1 expression in BAL cells isolated from 8-week old animals. Data represent mean ± SEM, n≥4, ★ $p<0.05$.

Figure 3

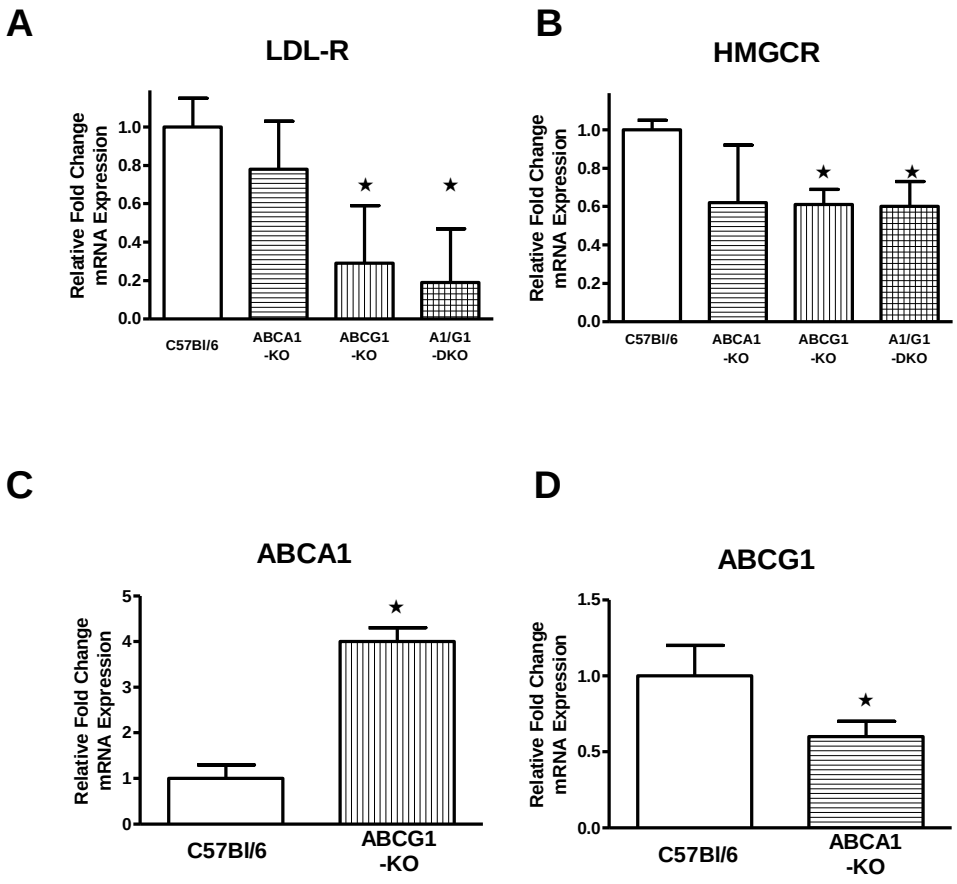
A
LDL-R
Relative Fold Change mRNA Expression
1.0
0.8
0.6
0.4
0.2
0.0
C57Bl/6
ABCA1 -KO
ABCG1 -KO
A1/G1 -DKO
B
HMGCR
Relative Fold Change mRNA Expression
C57Bl/6
ABCA1 -KO
ABCG1 -KO
A1/G1 -DKO
C
ABCA1
Relative Fold Change mRNA Expression
5
4
3
2
1
0
C57Bl/6
ABCG1 -KO
D
ABCG1
Relative Fold Change mRNA Expression
1.5
1.0
0.5
0.0
C57Bl/6
ABCA1 -KO

Figure 4: ABCG1 Deficiency Promotes Pulmonary Dyslipidemia. (A) Mean diameter of alveolar macrophages determined from BAL cell cytospins. (B) Total cholesterol and (C) cholesterol ester content of BAL fluid (BALF). Data represent mean ± SEM, n≥3, ★ $p<0.05$.

Figure 4

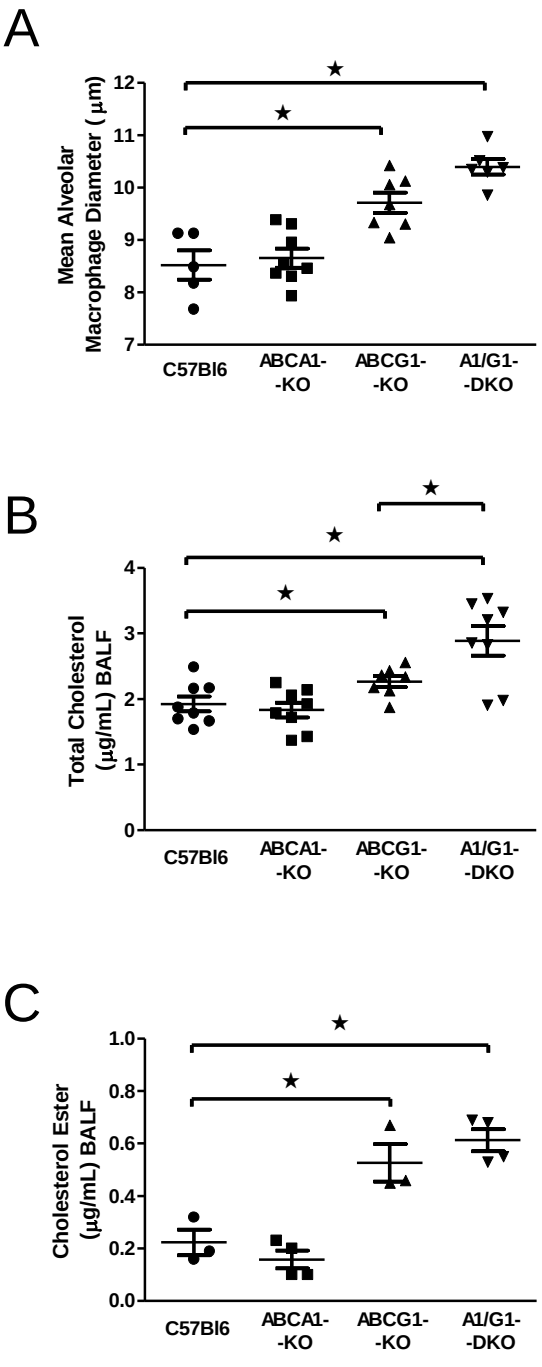
A
Mean Alveolar Macrophage Diameter (μm)
12
11
10
9
8
7
C57Bl6
ABCA1--KO
ABCG1--KO
A1/G1--DKO
B
Total Cholesterol (μg/mL) BALF
4
3
2
1
0
C57Bl6
ABCA1--KO
ABCG1--KO
A1/G1--DKO
C
Cholesterol Ester (μg/mL) BALF
1.0
0.8
0.6
0.4
0.2
0.0
C57Bl6
ABCA1--KO
ABCG1--KO
A1/G1--DKO

Figure 5: BAL cell Inflammatory Gene Expression of ABC-knockout Mice. Quantitative-PCR analysis of (A) CCL2 and (B) osteopontin expression in BAL cells isolated from naive 8-week old animals. Data represent mean ± SEM, n≥4, ★ $p<0.05$.

Figure 5

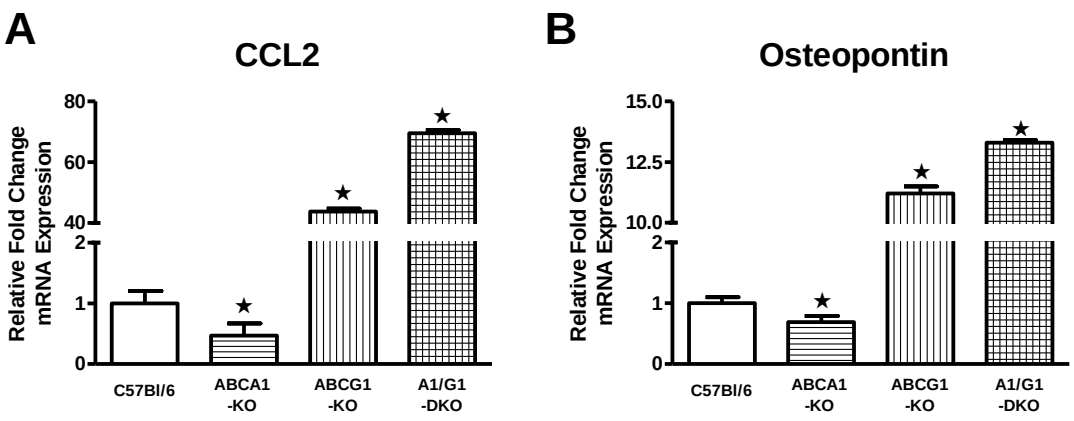
A
CCL2
Relative Fold Change mRNA Expression
80
60
40
2
1
0
C57Bl/6
ABCA1 -KO
ABCG1 -KO
A1/G1 -DKO
B
Osteopontin
Relative Fold Change mRNA Expression
15.0
12.5
10.0
2
1
0
C57Bl/6
ABCA1 -KO
ABCG1 -KO
A1/G1 -DKO

CHAPTER THREE

ALVEOLAR MACROPHAGE ABCG1 DEFICIENCY PROMOTES GRANULOMA FORMATION IN A CARBON NANOTUBE INDUCED MURINE MODEL OF SARCOIDOSIS

ABSTRACT

Pulmonary granuloma formation is a complex and poorly understood response to inhaled pathogens and particulate matter. To explore mechanisms of pulmonary granuloma formation and maintenance our laboratory has developed a multi-wall carbon nanotube (MWCNT) induced murine model of chronic granulomatous inflammation. We have demonstrated that the MWCNT model closely mimics pulmonary sarcoidosis pathophysiology, including the deficiency of alveolar macrophage ATP-binding cassette (ABC) lipid transporters ABCA1 and ABCG1. We hypothesized that deficiency of alveolar macrophage ABCA1 and ABCG1 would promote pulmonary granuloma formation and inflammation. To test this hypothesis, the effects of MWCNT instillation were evaluated in ABCA1, ABCG1 and ABCA1/ABCG1 macrophage-specific knockout mice. Histological examination found significantly larger pulmonary granulomas in ABCG1-KO and ABCA1/ABCG1 double knockout animals when compared to wild-type controls. Evaluation of bronchoalveolar lavage cells found increased expression of CCL2 and osteopontin, genes shown to be involved in the formation and maintenance of pulmonary granulomas. Deficiency of alveolar macrophage ABCA1 did not affect MWCNT induced granuloma formation or pro-inflammatory gene expression. These observations suggest that the deficiency of alveolar macrophage ABCG1 and, to a further extent, ABCA1 and ABCG1 promotes pulmonary granulomatous inflammation.

INTRODUCTION

Sarcoidosis is a chronic inflammatory condition characterized by the presence of non-necrotizing granulomas. While any organ can be affected, the lungs and mediastinal lymph nodes are involved in more than 90% of clinical cases [23]. Diagnosis is dependent on excluding the presence of infectious agents or previous exposure to materials known to produce granulomatous lesions. While the etiology of sarcoidosis remains unclear, current understanding suggests the presence of a poorly soluble antigen in genetically susceptible individuals. Epidemiological studies have found an association between the incidence of sarcoidosis and exposure to wood-burning stoves, fireplaces and certain occupations, such as firefighting [68;75;114]. These environments contain particulate matter of respirable sizes, particularly carbon nanotubes.

Carbon nanotubes are produced as the byproducts of combustion or manufactured for use in industrial processes. These materials may also have adverse implications for human health. Assessing the respiratory toxicology of carbon nanomaterials, Lam et al. observed granulomatous like lesions in the lungs of exposed animals [79]. These observations prompted our laboratory to investigate the use of multiwall carbon nanotubes (MWCNT) to generate a murine model of pulmonary sarcoidosis [58]. Our previous studies have shown that the MWCNT model bears striking similarities to sarcoidosis pathophysiology, including increased expression of pro-inflammatory mediators and decreased expression of alveolar macrophage ATP-binding cassette (ABC) lipid transporters ABCA1 and ABCG1 [16].

ABCA1 and ABCG1 facilitate the transfer of lipids across plasma membranes and play an important role in the catabolism of pulmonary surfactant. Deficiency of either ABCA1 or ABCG1 has been found to promote pulmonary lipid accumulation [11;19]. Intracellular lipid accumulation has been shown to promote pro-inflammatory macrophage activation [147]. Clinically, deficiency of lipid transporters have been observed in Tangiers disease (ABCA1) and pulmonary alveolar proteinosis (ABCG1). These pathologies are characterized by dysregulated lipid homeostasis and increased inflammatory mediators [26;131]. Upregulation of alveolar macrophage ABCG1 in a murine model of alveolar proteinosis has been shown to reduce pulmonary lipid accumulation and to improve lung function [87].

These observations suggest the lipid transporters ABCA1 and ABCG1 may play a significant role in pulmonary granulomatous inflammation. To further address this question we utilized macrophage-specific knockout (KO) mice, deficient in ABCA1, ABCG1 or both ABCA1 and ABCG1. We hypothesized that deficiency of the ABC-lipid transporters would exacerbate MWCNT induced granulomatous inflammation.

MATERIALS AND METHODS

Mice: All studies were conducted in accordance with the National Institutes of Health guide for the use of laboratory animals and approved by the East Carolina University Institutional Animal Care and Use Committee**.** C57Bl/6J wild-type mice were obtained from The Jackson Laboratory (Bar Harbor, ME). Generation of macrophage-specific ATP-binding cassette (ABC) lipid transporter knockout mice are described in Chapter 2. The instillation of multiwall carbon nanotubes (MWCNT) was performed as described previously [58]. Briefly, MWCNT were suspended in 35% Infasurf/phosphate buffered saline (vehicle) solution by ultrasonification. Animals were anesthetized using isoflorane, suspended by their incisors and oropharyngeally instilled with 50µL of vehicle or 100µg of MWCNT.

Tissue Collection: Animals were euthanized by intraperitoneal injection of tribromoethanol. Bronchoalveolar lavage (BAL) was performed by cannulating the trachea and sequentially lavaging the whole lung with 1mL aliquots of 0.2% lidocaine/PBS solution totaling 5mL as previously described [88]. Following centrifugation (1800 RPM x 10 minutes, 4°C), supernatant was snap frozen on dry ice as BAL fluid (BALF). BAL cells were washed twice in 4mL chilled PBS and snap frozen as a pellet for further analysis. Differential cell counts were determined from BAL cell cytospins, generated by centrifugation at 500 RPM x 5 minutes and subsequently stained with Diff Quick solution (Thermo Fisher Scientific. Waltham, MA). Histological analysis was performed on paraffin sections of whole lungs which had been inflated with 300µL 10% buffered formalin solution as previously described [58].

RNA Purification and Analysis: Total RNA was collected using the miRNeasy Micro Kit (Qiagen. Hilden, Germany) according to the manufacturer's protocol. Specific primers were obtained from Qiagen for ATP binding cassette (ABC) transporter-A1 (Abca1, PPM03952F), Abcg1 (PPM03895A), chemokine (C-C motif) ligand-2 (Ccl2, PPM03151G), Glyceraldehyde-3-phosphate-dehydrogenase (Gapdh, PPM02946E), osteopontin (Spp1, PPM03648C) platelet derived growth factor, alpha (Pdgfa, PPM03103E) and transforming growth factor, beta 1 (Tgfb1, PPM02991B). Relative gene expression of complimentary DNA synthesized with the RT2 First Strand Kit (Qiagen. Hilden, Germany) was evaluated on the StepOnePlus PCR system (Thermo Fisher Scientific. Waltham, MA) in comparison to Gapdh using the $2^{-\Delta\Delta CT}$ method [82].

Analysis of Bronchoalveolar Lavage Fluid: Total cholesterol content was measured using the Amplex Red Cholesterol Assay kit (Thermo Fisher Scientific. Waltham, MA) according to manufacturer's instructions in the presence of cholesterol esterase. The concentration of platelet derived growth factor subunit a (PDGFα) was determined using RayBio® Mouse PDGF-AA ELISA Kit (RayBioTech, cat# ELM-PDGFAA. Norcross, GA.) according to the manufacturer's instructions. The concentration of transforming growth factor beta (TGFβ) was determined using the LEGEND MAX Total TGF-β1 ELISA Kit (BioLegend, cat#436707. San Diego, CA) according to the manufacturer's instructions.

Histological Assessment: Following fixation, entire mouse lungs were embedded in paraffin. Five-micron thick sections were stained with hematoxylin & eosin (H&E) or Gomori's trichrome. Quantitative analysis of granulomas were performed on digital images of H&E stained whole lung sections acquired on an Aperio ScanScope (Aperio

Technologies, Inc. Vista, CA). Analysis was performed blindly on randomized digital images, scanning the entire lung at 20X magnification for pulmonary granulomas. A granuloma was defined as a carbon aggregate completely surrounded by tissue and associated with three or more cell nuclei. Pulmonary fibrosis scoring was performed using modified Ashcroft method [57] and represents the mean score of 40 randomly chosen fields (X200 magnification) across the entire lung. The length (L) and width (W) of the tracheobronchal lymph node, identified based on Van den Broeck et al. [133], was used to determine lymph node volume using the formula $(LxW^2)\pi/6$. Carbon content of alveolar macrophages was determined by evaluating alveolar macrophages on BAL cytospins described above under 400X magnification.

Phagocytosis Assay: Phagocytic ability of alveolar macrophages was evaluated using the pHrodo BioParticles Phagocytosis Flow Cytometry Kit (Thermo Fisher Scientific. Waltham, MA) according to manufacturer's protocol. The identification of alveolar macrophages was facilitated by counterstaining the cells with anti-CD11c. Alveolar macrophages were defined as $CD11c^+$ cells.

Statistical Analysis: All data represent the mean of at least three individual experiments ±SEM unless otherwise indicated. Statistical analysis was performed using Graph Pad Prism software (San Diego, CA). Significance was determined by using unpaired Student's t-test (2 groups) or ANOVA (>2 groups) followed by Bonferroni correction. A confidence interval of $p<0.05$ was considered statistically significant.

RESULTS

Macrophage ABCG1 Deficiency Promotes Pulmonary Granuloma Formation

To evaluate the effects of alveolar macrophage lipid transporter deficiency on pulmonary granuloma formation, macrophage-specific ABCA1, ABCG1 or ABCA1/ABCG1 double knockout mice were utilized. Animals were evaluated 60 days following instillation of vehicle (35% surfactant) or 100μg of MWCNT. Wild-type C57Bl/6 and ABCA1-KO animals instilled with vehicle were histologically indistinguishable (Figure 1). Vehicle instilled ABCG1-KO or ABCA1/ABCG1-DKO mice however exhibited a marked increase of lipid loaded alveolar macrophages within the airways. These observations are similar to previous observations in ABCG1 deficient animals [11]. Following MWCNT instillation, pulmonary granulomas in C57Bl/6 and ABCA1-KO mice typically consisted of a carbon aggregate core surrounded by epithelioid macrophages (Figure 1). Granulomas in ABCG1-KO and ABCA1/ABCG1-DKO animals were noticeably different, generally consisting of multiple carbon aggregates and irregular boarders of epithelioid macrophages. Representative images are shown in Figure 1.

Granulomatous inflammation was further characterized by determining the average number and size of MWCNT induced lesions from digital images of H&E stained lung sections. Our analysis found the average number of granulomas per whole lung section was similar between ABC-lipid transporter knockouts and wild-type animals (Figure 2A). Evaluation of mean granuloma size found a slight, but non-significant increase in ABCA1-KO granulomas (Figure 2B). MWCNT induced granulomas observed in ABCG1-KO and ABCA1/ABCG1-DKO animals however were found to be

35% and 39% larger, respectively, than those observed in wild-type controls (Figure 2B).

Macrophage ABCG1 Deficiency Promotes Alveolar Macrophage Inflammatory Gene Expression.

To determine if the alveolar cell population was affected by MWCNT, bronchoalveolar lavage (BAL) was performed 60 days following instillation. Wild-type and ABCA1-KO BAL consisted of approximately $1.0x10^6$ leukocytes and were predominately alveolar macrophages, (>97%) (Figure 3). ABCG1-KO and ABCA1/ABCG1-DKO had twice as many isolated leukocytes, (~$2.0x10^6$), compared to wild-type animals and, as previously observed [143], included increased polymorphonuclear cells, (9-16%) (Figure 3B). The total cell count nor composition of leukocytes in the lavage were affected by the instillation of MWCNT when compared to vehicle instilled animals (Figure 3).

Previous studies have found the pro-inflammatory mediators (C-C motif) ligand-2 (CCL2) and osteopontin play a critical role in the formation of pulmonary granulomas [83;104]. Our laboratory has also reported the upregulation of these genes in BAL cells isolated from MWCNT instilled wild-type animals [15;59]. The data reported here are similar to those observations. The deficiency of ABCA1 did not promote CCL2 or osteopontin expression following MWCNT instillation (Figure 4). Vehicle-instilled ABCG1-KO animals exhibited significantly higher CCL2 and osteopontin expression compared to wild-type animals, and this increase was further exacerbated by the instillation of MWCNT (Figure 4). Interestingly, BAL cells of vehicle-instilled ABCA1/ABCG1-DKO animals demonstrated significantly higher CCL2 and osteopontin

expression than ABCG1-KO, but had no additional increase of these genes following MWCNT instillation (Figure 4).

ABCG1 Deficiency Promotes MWCNT Induced Fibrosis and Pro-Fibrotic Mediators

The progression of pulmonary sarcoidosis is frequently characterized by the development of fibrosis. MWCNT induced fibrosis was evaluated from whole lung sections following Gomori trichrome staining. We have previously reported that the MWCNT induced granulomas of wild-type animals do not consistently demonstrate collagen deposition [58]. Here we sought to increase the sensitivity of our analysis by evaluating the entire lung. Using this method, we found that MWCNT instilled wild-type animals have increased fibrosis compared to those receiving vehicle alone (Figure 5A). MWCNT instilled ABCA1-KO animals demonstrate a similar increase in fibrosis score compared to wild-type animals (Figure 5A). ABCG1-KO and ABCA1/ABCG1-DKO animals instilled with vehicle demonstrate a significantly higher fibrosis score than wild-type animals, and this increase was further exacerbated by the instillation of MWCNT (Figure 5A). MWCNT induced fibrosis in both ABCG1-KO and ABCA1/ABCG1-DKO mice was significantly greater than that observed in wild-type animals.

To further examine fibrotic changes, we evaluated alveolar macrophage gene expression and BAL fluid protein concentration of the pro-fibrotic mediators' platelet derived growth factor-α (PDGFα) and transforming growth factor-β (TGFβ). We found that BAL cells from wild-type and ABCA1-KO animals demonstrate a similar increase in PDGFα expression following MWCNT instillation (Figure 5B). Vehicle-instilled ABCG1-KO and ABCA1/ABCG1-DKO BAL cells had significantly higher PDGFα mRNA expression than wild-type animals, and demonstrate a further increase following

MWCNT instillation (Figure 5B). The combined deficiency of ABCA1/ABCG1 did not further promote BAL cell PDGFα expression. Evaluation of BAL cell TGFβ expression found no difference between vehicle instilled wild-type or ABC-lipid transporter knockout animals (Figure 5C). Following MWCNT instillation we observed a slight increase of TGFβ expression in BAL cells of ABCG1-KO (1.2 ± 0.2 fold) and ABCA1/ABCG1-DKO (1.2 ± 0.1 fold) animals compared with vehicle instilled controls (Figure 5C). TGFβ expression did not statistically differ between MWCNT instilled wild-type, ABCG1-KO or ABCA1/ABCG1-DKO animals.

Further evaluation of BAL fluid PDGFα protein concentration found no significant difference between vehicle instilled wild-type (64.6±13.2 pg/mL), ABCA1-KO (42.6±10.2 pg/mL), ABCG1-KO (71.1±7.2 pg/mL) or ABCA1/ABCG1-DKO (57.4±2.0 pg/mL) animals. Following MWCNT instillation, BAL fluid PDGFα concentration was elevated in wild-type (104.6±11.6 pg/mL, p=0.06), ABCA1-KO (89.6±8.9 pg/mL), ABCG1-KO (116.1±8.1 pg/mL) and ABCA1/ABCG1-DKO animals (135.4±20.3 pg/mL) animals (Figure 5D). BAL fluid PDGFα protein concentration did not statistically differ between MWCNT instilled wild-type and ABC-lipid transporter knockout animals. BAL fluid TGFβ protein concentrations of vehicle instilled wild-type (31.0±1.9 pg/mL) and ABCA1-KO (27.5±1.8 pg/mL) animals were not statistically different. However, in contrast to BAL cell gene expression, TGFβ protein concentration of the BAL fluid was significantly higher in ABCG1-KO (349.5±58.9 pg/mL) and ABCA1/ABCG1-DKO (348.9±39.7 pg/mL) animals when compared to wild-type mice (Figure 5E). Following MWCNT instillation, we observed a slight increase of TGFβ protein concentration in wild-type (85.6±16.6 pg/mL) and ABCA1-KO (73.1±34.0 pg/mL) animals (Figure 5E). MWCNT instilled

ABCG1-KO (304.1±46.6 pg/mL) and ABCA1/ABCG1-DKO (341.9±36.7 pg/mL) animals demonstrated constitutively higher TGFβ protein content than wild-type animals, but were not statistically different from vehicle instilled controls (Figure 5E).

Instillation of MWCNT Differentially Regulates the Expression of Lipid Transporters

The effects of MWCNT instillation were evaluated on the expression of the remaining lipid transporter in single-knockout animals. ABCG1-mRNA was reduced in ABCA1-KO animals following MWCNT instillation, similar to changes observed in wild-type mice [16], (Figure 6A). In contrast, MWCNT instillation increased the expression of ABCA1-mRNA in ABCG1-KO animals (Figure 6B). Changes in pulmonary lipid composition were evaluated by measuring the total cholesterol content of the BAL fluid. We found BAL fluid cholesterol concentration of vehicle-instilled wild-type (1.6 ± 0.1μg/mL) and ABCA1-KO (1.5 ± 0.1μg/mL) animals did not differ, however ABCG1-KO (2.9 ± 0.3μg/mL) and ABCA1/ABCG1-DKO (4.6 ± 0.6μg/mL) animals showed progressive lipid accumulation in the lungs (Figure 7). Following MWCNT instillation, BAL fluid cholesterol was significantly increased in wild-type (2.3 ± 0.2μg/mL) and ABCA1-KO mice (2.4 ± 0.4μg/mL). The increased BAL fluid cholesterol content observed in ABCG1-KO (3.5 ± 0.3μg/mL) or ABCA1/ABCG1-DKO (6.0 ± 1.0μg/mL) mice failed to reach significance compared to vehicle controls, but were significantly greater than in MWCNT instilled wild-type animals (Figure 7).

ABC-Lipid Transporter Deficient Alveolar Macrophages have Increased Carbon Content and Phagocytic Capacity

The observations that ABCG1 deficiency promotes alveolar macrophage activation and MWCNT induced granulomatous inflammation prompted us to further investigate how these cells phagocytose carbon nanoparticles. We hypothesized that ABCG1 deficiency would lead to a greater number of carbon containing alveolar macrophages. To test this hypothesis, alveolar macrophages were evaluated from BAL cell cytospins for the presence or absence of intracellular carbon. We found that the percentage of alveolar macrophages containing carbon were significantly higher in each ABC-lipid transporter knockout: ABCA1-KO (26 ± 3.4%), ABCG1-KO (22 ± 2.2%) and ABCA1/ABCG1-DKOs (22 ± 1.5%) compared to wild-type (14 ± 1.4%) animals (Figure 8). While no significant difference was observed among ABCA1, ABCG1 or ABCA1/ABCG1 knockouts, the increased percentage of ABCA1-KO macrophages containing carbon was unexpected.

To further define the phagocytic capacity of ABC-lipid transporter deficient alveolar macrophages, BAL cells were incubated with pH-sensitive fluorescently labeled *E.coli* particles and evaluated by flow cytometry (Figure 9). The percentage of alveolar macrophages which phagocytized labeled particles was increased in ABCA1-KO (35 ± 1.9%) and to a further extent, in ABCG1-KO (55 ± 2.5%) and ABCA1/ABCG1-DKO (51 ± 2.6%), compared to wild-type (24 ± 4.2%) animals (Figure 9B). Mean florescent intensity, a measure of the number of particles phagocytosed per macrophage, was significantly increased in ABCG1-KO and ABCA1/ABCG1-DKO animals, but not

ABCA1-KO (Figure 9D). These data agree with a previous report which found that ABCG1 deficient macrophages had an increased capacity to clear apoptotic cells [143].

MWCNT Induced Mediastinal Lymphadenopathy is Exacerbated by the Deficiency of ABC-Lipid Transporters.

Mediastinal and hilar lymph node involvement are defining characteristics of pulmonary sarcoidosis. Previous studies have shown the ability of intra-tracheally instilled MWCNT to translocate to lung associated lymph nodes [2]. We sought to characterize the change in mediastinal lymph node volume in wild type and ABC-lipid transporter deficient animals following MWCNT instillation. The lymph node volume of vehicle-instilled wild-type (1.8 ± 0.2 mm^3) and ABCA1-KO (2.0 ± 0.2 mm^3) animals did not statistically differ; however ABCG1-KO (6.6 ± 0.9 mm^3) and ABCA1/ABCG1-DKO (10.6 ± 1.2 mm^3) animals had a significant increase in lymph node volume. Following MWCNT instillation, mediastinal lymph node volume was significantly increased in wild-type (4.8 ± 0.4 mm^3), ABCA1-KO (5.5 ± 0.7 mm^3), ABCG1-KO (9.7 ± 0.9 mm^3) and ABCA1/ABCG1-DKO (15.5 ± 1.2 mm^3) compared to vehicle-instilled controls. The MWCNT induced mediastinal lymphadenopathy observed in ABCG1-KO and ABCA1/ABCG1-DKO mice was significantly greater than wild-type animals (Figure 10).

DISCUSSION

We have previously described a MWCNT induced model of chronic granulomatous inflammation which bears striking similarity to pulmonary sarcoidosis, including the deficiency of alveolar macrophage lipid transporters ABCA1 and ABCG1 [16;58]. The deficiency of these genes correlate with pulmonary lipid accumulation and increased expression of pro-inflammatory mediators in the MWCNT model [13;16]. While the deficiency of ABCA1 or ABCG1 has been shown to promote pulmonary lipid accumulation [10;19], the involvement of these transporters in chronic granulomatous lung disease remains unclear. These studies aimed to determine if the deficiency of ABCA1 or ABCG1 contributes to pulmonary granuloma formation and inflammation. Here we report that deficiency of alveolar macrophage ABCG1, but not ABCA1, promotes MWCNT induced pulmonary granuloma formation, pulmonary fibrosis, pro-fibrotic mediators and the expression of CCL2 and osteopontin. These observations suggest that alveolar macrophage ABCG1 acts as a negative regulator of pulmonary granulomatous inflammation.

The pro-inflammatory mediators CCL2 and osteopontin are upregulated in granulomatous tissue of pulmonary sarcoidosis patients and wild-type animals bearing MWCNT induced granulomas [15;59;108]. Deficiency of these genes in murine studies has been shown to prevent the formation of pulmonary granulomas in response to stimuli [83;104], suggesting that these mediators play an integral role in the process. ABCG1 deficiency has been shown to promote pulmonary inflammation, including increased expression of CCL2 in lung tissue of total knockout animals [8]. To our knowledge, the expression of osteopontin has not been evaluated in the lungs of lipid

transporter deficient mice. Evaluation of CCL2 and osteopontin found intrinsic elevation of these mediators in in alveolar macrophages deficient of ABCG1 and further upregulation following MWCNT instillation. The increased expression of these mediators in ABCG1 or ABCA1/ABCG1 macrophage-specific knockout animals likely promotes MWCNT induced granuloma formation.

Here we report that deficiency of alveolar macrophage ABCG1 or the combined deficiency of ABCA1/ABCG1, promotes MWCNT induced lymphadenopathy, pulmonary fibrosis and the pro-fibrotic mediators PDGFα and TGFβ. These observations correlate with the progressive pulmonary lipid accumulation noted in these animals. Previous studies have reported lipid loaded macrophages in patients suffering from fibrotic lung disease and in animal models of pulmonary fibrosis [5;17;54;145]. Transcriptome analysis of lipid loaded macrophages isolated from subcutaneous granulomas revealed increased expression of pro-fibrotic pathways [130]. Furthermore, Romero et al. have demonstrated that deficiency of ABCG1, in part due to pulmonary lipidosis, promotes bleomycin induced lung fibrosis [118]. These observations further suggest a link between dysregulated pulmonary lipid homeostasis and the progression of lung diseases.

In an effort to better describe how ABC-lipid transporter deficient alveolar macrophages respond to carbon nanoparticles, we evaluated the carbon content and phagocytic capacity of these cells. We found an increased number of ABCA1, ABCG1 and ABCA1/ABCG1 deficient macrophages contain carbon compared to wild-type animals. Further studies demonstrate that the phagocytic ability of these cells increases in the order of: ABCA1/ABCG1-*DKO ≈ ABCG1-KO > ABCA1-KO > C57/Bl6 (wild-type).*

The increased number of carbon laden macrophages in ABCA1-KO BAL was unexpected. Given the increased total BAL cell count observed in the ABCG1 and ABCA1/ABCG1-DKO animals, it may be inferred that the macrophage-carbon ratio is decreased in these animals, explaining the relatively equal number of carbon containing macrophages in ABCA1-KO animals. While these studies do not account for unique mechanisms of E.coli and carbon nanotube phagocytosis, the observations suggest macrophage deficiency of ABCG1 or combined ABCA1/ABCG1 may promote carbon nanotube phagocytosis and retention in the lung, increasing pulmonary toxicity.

An unexpected observation made during the course of these studies was the absence of a significant increase in pro-inflammatory mediators in ABCA1-KO. Previous reports have found progressive pulmonary lipid accumulation in complete ABCA1-KO animals [19;90], but at a slower rate than observed in ABCG1 deficient animals. The absence of significant pulmonary lipid accumulation may explain the lack of an inflammatory phenotype. Previous studies have also indicated that the inflammatory potential of ABCA1 deficient macrophages is less than those deficient of ABCG1 or ABCA1/ABCG1. Following lipopolysaccharide (LPS) stimulation, peritoneal macrophages of ABCA1 deficient mice showed only a slight increase in a limited subset of inflammatory cytokines compared to ABCG1 or, to a greater extent, ABCA1/ABCG1-double knockout cells [147].

In conclusion, our studies indicate that alveolar macrophage ABCG1 is a crucial regulator of pulmonary granuloma formation and inflammation. Our laboratory has demonstrated that the MWCNT model closely mimics sarcoidosis pathophysiology. The progressive stages of pulmonary sarcoidosis are characterized by hilar node

involvement, granulomatous infiltrates into the lungs and finally end stage pulmonary fibrosis [137]. Here we demonstrate that the deficiency of alveolar macrophage ABCG1 exacerbates each of these clinical parameters. We have recently demonstrated that increased alveolar macrophage ABCG1 expression and inhibition of pulmonary lipid accumulation correlate with reduced MWCNT induced pulmonary granuloma formation [91]. These observations together with those from the current study suggest that alveolar macrophage ABCG1 may serve as a novel therapeutic target in granulomatous lung disease.

Figure 1: Representative Images or MWCNT Induced Granulomas. Representative images of C57Bl/6, ABCA1-KO, ABCG1-KO and ABCA1/ABCG1-DKO animals instilled with vehicle (X400) or MWCNT at low power (X100) or high power magnification (X400).

C57Bl/6
ABCA1-KO
ABCG1-KO
A1/G1-DKO
Vehicle (x400)
MWCNT (x100)
MWCNT (x400)

.

Figure 2: ABCG1 Deficiency Exacerbates the Size of Pulmonary Granulomatous Lesions. Quantitative analysis of the (A) number and (B) size of MWCNT induced granulomatous lesions observed from H&E stained lung tissue. Data represent mean ± SEM, ★ $p<0.05$, $n\geq6$.

Figure 2

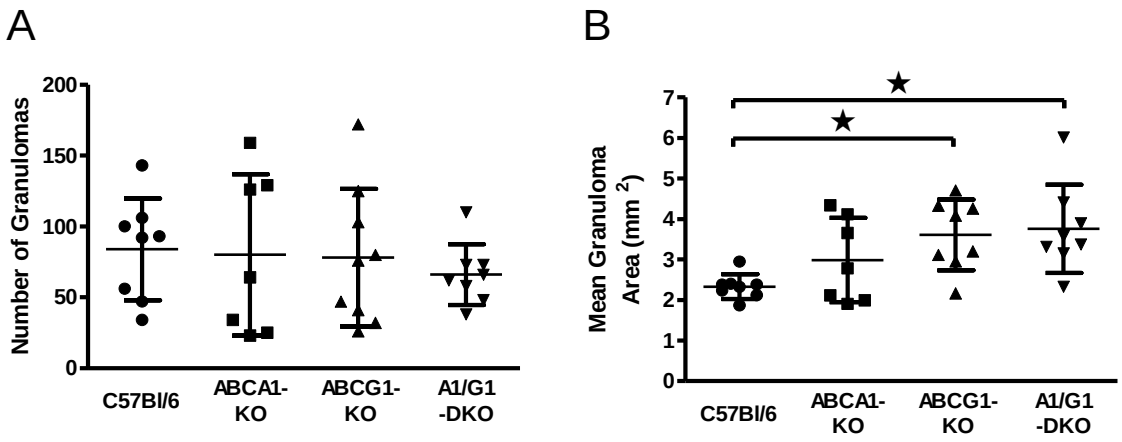
A
Number of Granulomas
200
150
100
50
0
C57Bl/6
ABCA1-KO
ABCG1-KO
A1/G1-DKO
B
Mean Granuloma Area (mm 2)
7
6
5
4
3
2
1
0
C57Bl/6
ABCA1-KO
ABCG1-KO
A1/G1-DKO

Figure 3: Macrophage ABCG1 Deficiency Promotes Inflammatory Cell Recruitment. (A) Total cell count and (B) differential cell counts of BAL 60 days following vehicle or MWCNT instillation. Data represent mean ± SEM, ★ $p<0.05$ $n\geq6$.

Figure 3

A

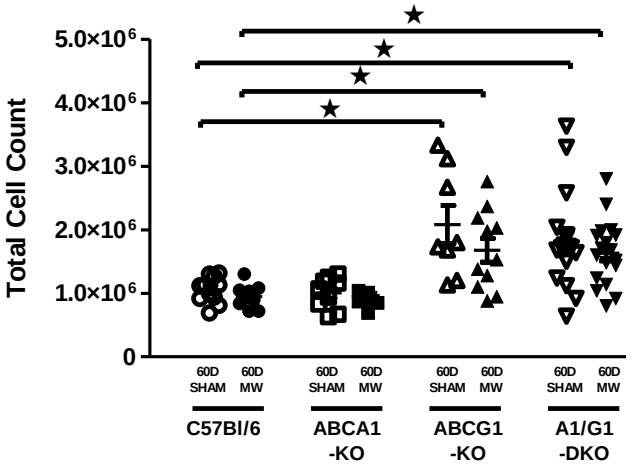

B

Strain/Treatment	AMs (%)	L (%)	PMN (%)
C57Bl/6			
Vehicle, n=11:	98.9±0.3	1.1±0.3	0
MWCNT, n=11:	99.6±0.4	1.1±0.4	0
ABCA1-KO			
Vehicle, n=9:	99.9±0.1	0.1±0.1	0
MWCNT, n=9:	97.3±0.7	0.7±0.3	2.3±0.7★
ABCG1-KO			
Vehicle, n=8:	89.5±2.2★	1.8±0.5	8.9±1.7★
MWCNT, n=11:	89.8±1.5★	1.0±0.4	9.5±1.3★
A1/G1-DKO			
Vehicle, n=16:	85.1±1.9★	1.9±0.5	13.1±1.5★♦
MWCNT, n=18:	82.8±1.6★	1.5±0.4	15.9±1.4★♦

***Definition of abbreviations**:* AMs: Alveolar Macrophage, L: Lymphocytes, PMN: Polymorphonuclear cell. ★ $p<0.05$ Knockout vs C57Bl/6, ♦ $p<0.05$ ABCG1-KO vs. A1/G1-DKO

Figure 4: Macrophage ABCG1 Deficiency Promotes Pro-Inflammatory Gene expression. Quantitative-PCR analysis of (A) CCL2 and (B) osteopontin expression in BAL cells of vehicle or MWCNT instilled animals. Data represent mean ± SEM, n≥4/treatment.

Figure 4

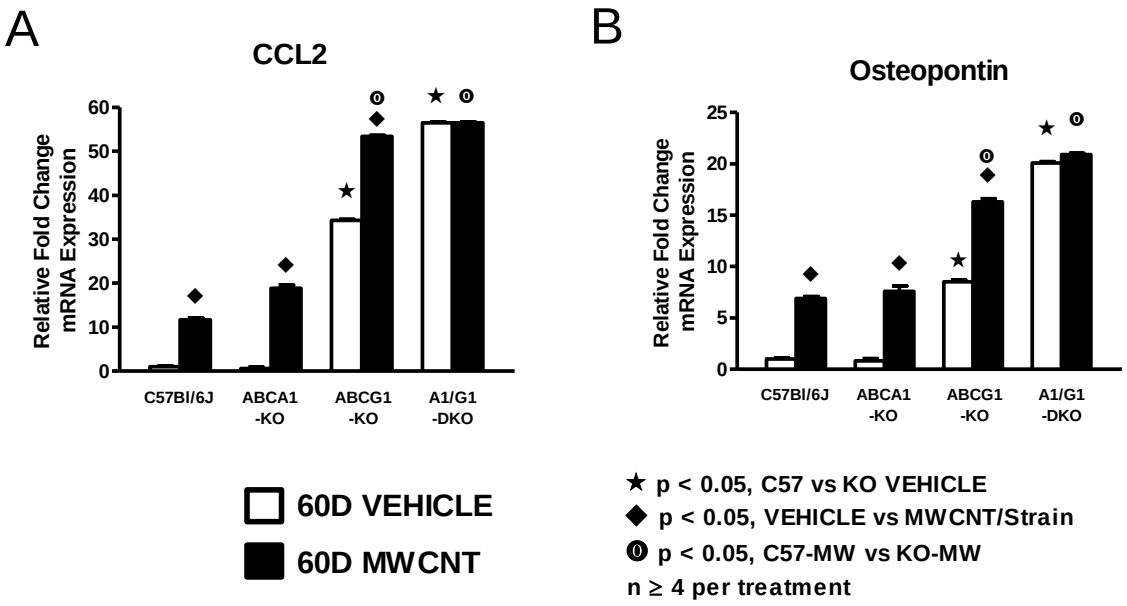
A
CCL2
Relative Fold Change mRNA Expression
60
50
40
30
20
10
0
C57Bl/6J
ABCA1 -KO
ABCG1 -KO
A1/G1 -DKO
60D VEHICLE
60D MWCNT
B
Osteopontin
Relative Fold Change mRNA Expression
25
20
15
10
5
0
C57Bl/6J
ABCA1 -KO
ABCG1 -KO
A1/G1 -DKO
★ p < 0.05, C57 vs KO VEHICLE
◆ p < 0.05, VEHICLE vs MWCNT/Strain
⓿ p < 0.05, C57-MW vs KO-MW
n ≥ 4 per treatment

Figure 5: Deficiency of ABCG1 Promotes Pulmonary Fibrosis. (A) Modified Ashcroft scoring of vehicle or MWCNT instilled whole lung sections. (B) qRT-PCR analysis of PDGFα expression in alveolar macrophages of vehicle or MWCNT instilled mice (★p < 0.05, C57-SHAM vs KO-SHAM; ◆ p < 0.05, SHAM vs MWCNT/Strain; ⓿ p < 0.05, C57-MW vs KO-MW, n≥4/treatment). The concentration of BAL fluid (C) PDGFα, (D) total TGF-β and (E) active TGF-β. Data represent mean ± SEM, ★ p<0.05.

Figure 5

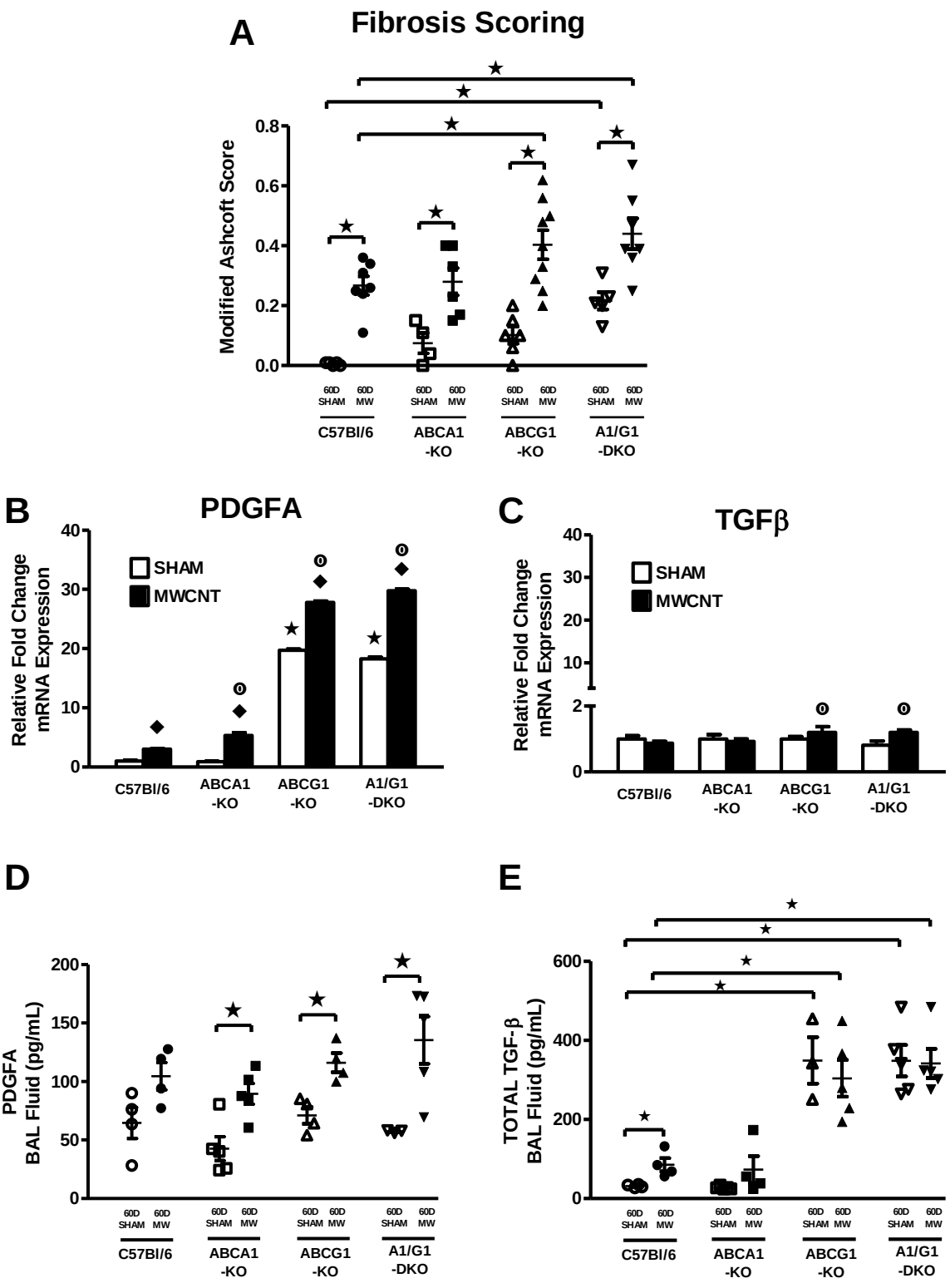
A
Fibrosis Scoring
Modified Ashcoft Score
0.0
0.2
0.4
0.6
0.8
60D SHAM
60D MW
C57Bl/6
ABCA1 -KO
ABCG1 -KO
A1/G1 -DKO
B
PDGFA
Relative Fold Change mRNA Expression
SHAM
MWCNT
0
10
20
30
40
C57Bl/6
ABCA1 -KO
ABCG1 -KO
A1/G1 -DKO
C
TGFβ
Relative Fold Change mRNA Expression
SHAM
MWCNT
0
2
10
20
30
40
C57Bl/6
ABCA1 -KO
ABCG1 -KO
A1/G1 -DKO
D
PDGFA BAL Fluid (pg/mL)
0
50
100
150
200
60D SHAM
60D MW
C57Bl/6
ABCA1 -KO
ABCG1 -KO
A1/G1 -DKO
E
TOTAL TGF-β BAL Fluid (pg/mL)
0
200
400
600
60D SHAM
60D MW
C57Bl/6
ABCA1 -KO
ABCG1 -KO
A1/G1 -DKO

Figure 6: Instillation of MWCNT affects ABC-Lipid Transporter Expression. Quantitative-PCR analysis of (A) ABCG1 expression in ABCA1-KO animals and ABCA1 expression in ABCG1-KO animals 60 days following instillation of vehicle or MWCNT. Data represent mean ± SEM, n≥4/treatment.

Figure 6

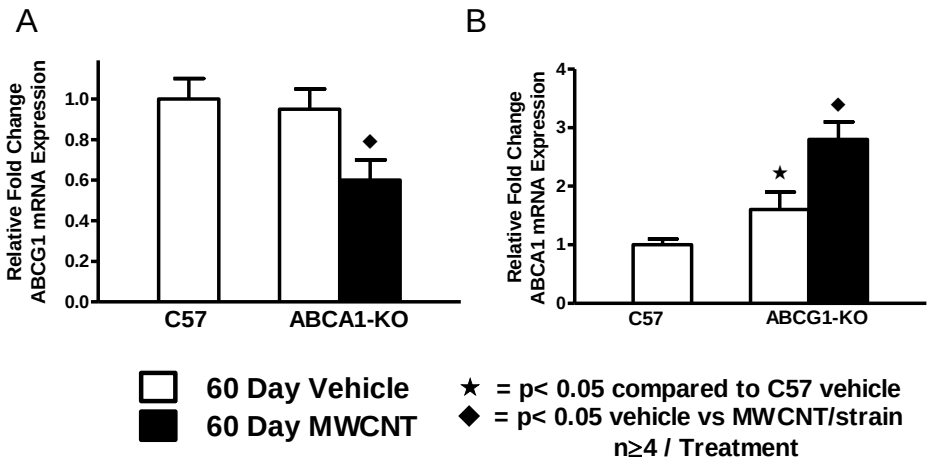
A
B
Relative Fold Change ABCG1 mRNA Expression
1.0
0.8
0.6
0.4
0.2
0.0
C57
ABCA1-KO
Relative Fold Change ABCA1 mRNA Expression
4
3
2
1
0
C57
ABCG1-KO
60 Day Vehicle
60 Day MWCNT
★ = p< 0.05 compared to C57 vehicle
◆ = p< 0.05 vehicle vs MWCNT/strain
n≥4 / Treatment

Figure 7: Pulmonary Lipid Accumulation is elevated in ABCG1 and ABCA1/ABCG1 deficient animals. Total cholesterol content of BAL fluid 60 days following instillation of vehicle or MWCNT was evaluated. Data represent mean ± SEM, ★ $p<0.05$.

Figure 7

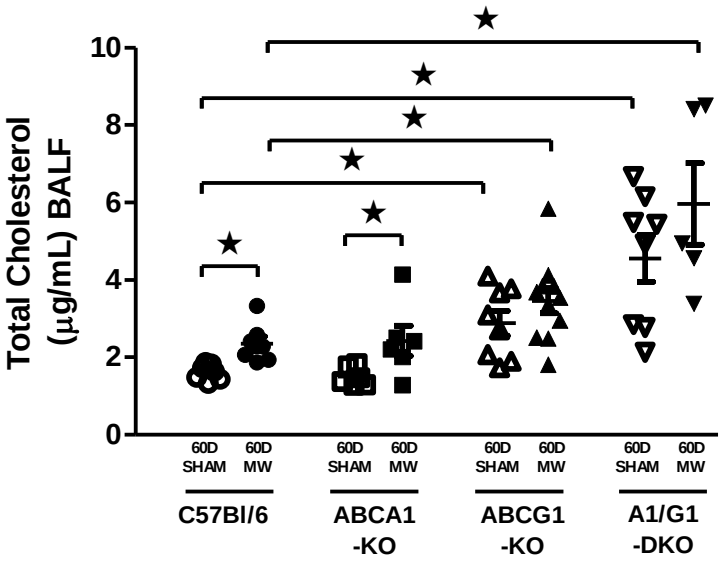
Total Cholesterol (μg/mL) BALF
10
8
6
4
2
0
60D SHAM
60D MW
C57Bl/6
ABCA1 -KO
ABCG1 -KO
A1/G1 -DKO

Figure 8: Percentage of Alveolar Macrophages Containing MWCNT. Alveolar macrophages of wild type or ABC-knockout mice were visualized on BAL cell cytospins (400X) and evaluated for the presence of MWCNT. Data represent mean ± SEM, ★ $p<0.05$.

Figure 8

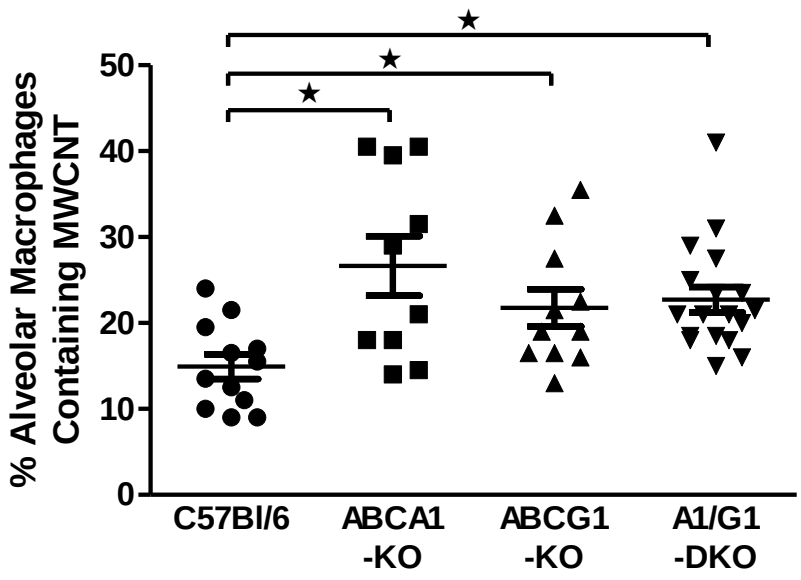
% Alveolar Macrophages Containing MWCNT
50
40
30
20
10
0
C57Bl/6
ABCA1 -KO
ABCG1 -KO
A1/G1 -DKO

Figure 9: Phagocytic Capacity of Lipid Transporter Deficient Alveolar Macrophages. (A) Representative contour plots of flow cytometry data. (B) Percent alveolar macrophage population to phagocytose fluorescently labeled *E.coli* particle. (C) Representative mean florescent intensity per alveolar macrophage. (D) Mean florescent intensity of alveolar macrophage population. Data represent mean ± SEM. ★=$p<0.02$, $n\geq5$.

Figure 9

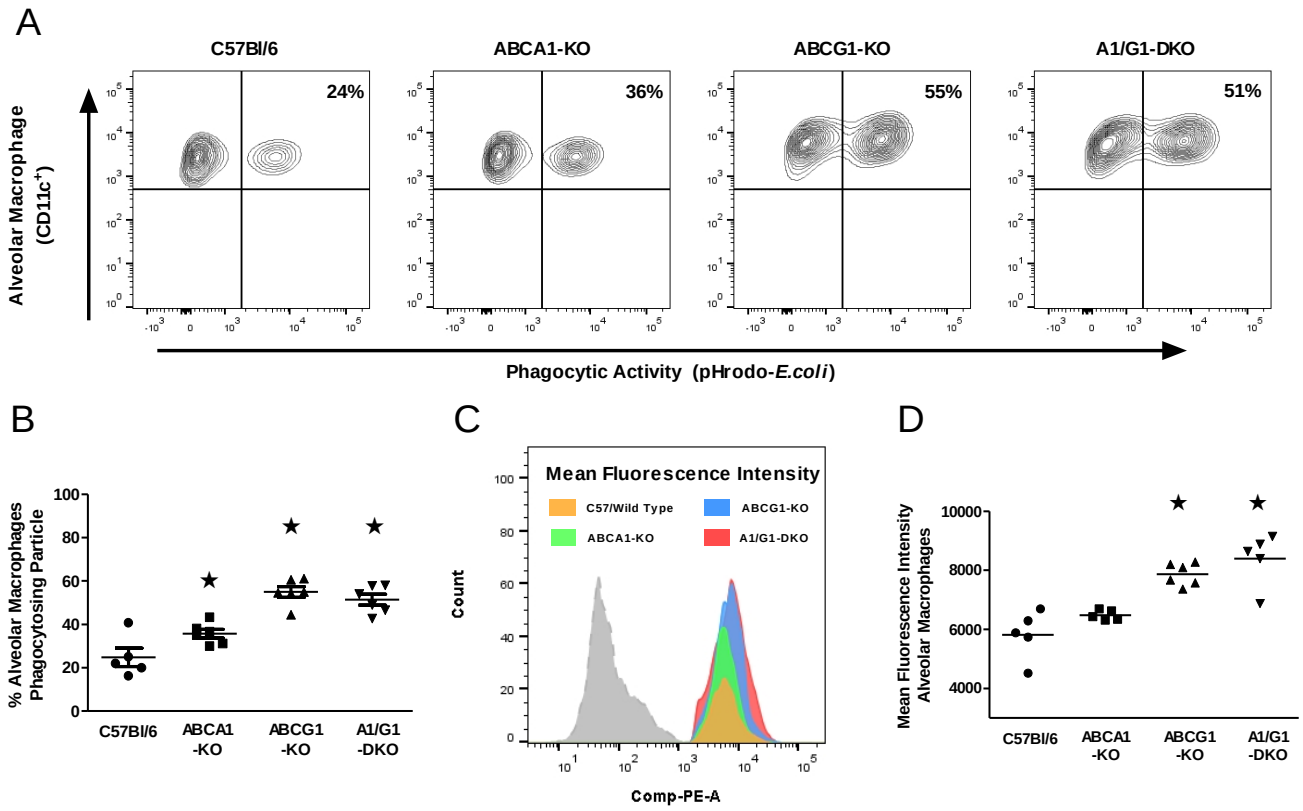
A
C57Bl/6
ABCA1-KO
ABCG1-KO
A1/G1-DKO
24%
36%
55%
51%
Alveolar Macrophage (CD11c+)
Phagocytic Activity (pHrodo-E.coli)
B
% Alveolar Macrophages Phagocytosing Particle
C57Bl/6
ABCA1 -KO
ABCG1 -KO
A1/G1 -DKO
C
Mean Fluorescence Intensity
C57/Wild Type
ABCG1-KO
ABCA1-KO
A1/G1-DKO
Count
Comp-PE-A
D
Mean Fluorescence Intensity Alveolar Macrophages

Figure 10: MWCNT Induced Lymphadenopathy is Exacerbated by the Deficiency of ABCG1. Mediastinal lymph node volume was determined from mice 60 days following instillation of vehicle or MWCNT. Data represent mean ±SEM, ★=$p<0.02$, n≥6/treatment.

Figure 10

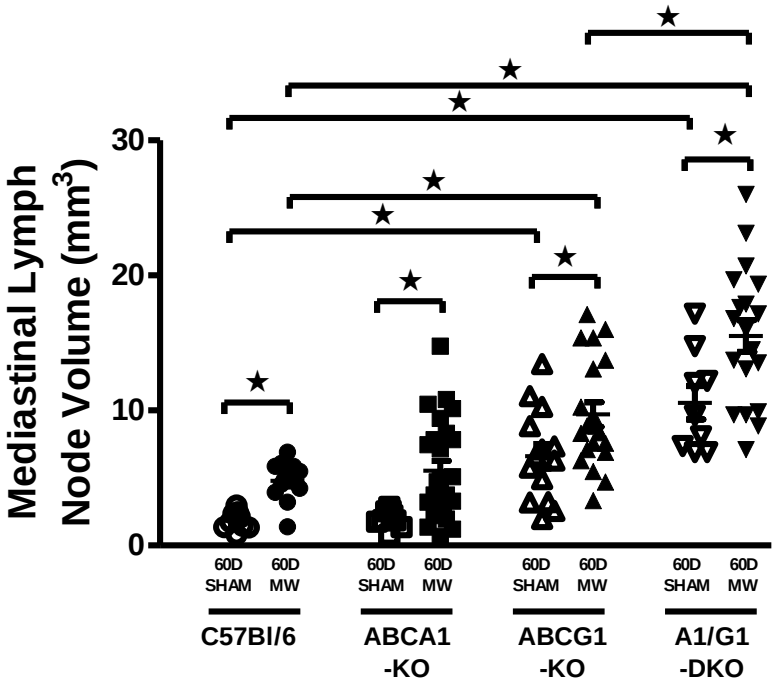
Mediastinal Lymph Node Volume (mm3)
30
20
10
0
60D SHAM
60D MW
60D SHAM
60D MW
60D SHAM
60D MW
60D SHAM
60D MW
C57Bl/6
ABCA1 -KO
ABCG1 -KO
A1/G1 -DKO

CHAPTER 4

PPAR-GAMMA PATHWAYS ATTENUATE PULMNARY GRANULOMA FORMATION IN A CARBON NANOTUBE INDUCED MURINE MODEL OF SARCOIDOSIS

ABSTRACT

Peroxisome proliferator activated receptor gamma (PPARγ), a ligand activated nuclear transcription factor, is constitutively expressed in alveolar macrophages of healthy individuals. PPARγ deficiencies have been noted in several lung diseases including the alveolar macrophages of pulmonary sarcoidosis patients. We have previously described a murine model of multiwall carbon nanotube (MWCNT) induced pulmonary granulomatous inflammation which bears striking similarities to pulmonary sarcoidosis, including the deficiency of alveolar macrophage PPARγ. Further studies demonstrate alveolar macrophage PPARγ deficiency exacerbates MWCNT induced pulmonary granulomas. Based on these observations we hypothesized that activation of PPARγ via administration of the PPARγ-specific ligand rosiglitazone would limit MWCNT induced granuloma formation and promote PPARγ-dependent pathways. Results presented here show that rosiglitazone significantly limits the frequency and severity of MWCNT induced pulmonary granulomas. Furthermore, rosiglitazone attenuates alveolar macrophage NF-κB activity and downregulates the expression of the pro-inflammatory mediators, CCL2 and osteopontin. PPARγ activation via rosiglitazone also prevents the MWCNT induced deficiency of PPARγ-regulated ATP-binding cassette lipid transporter-G1 (ABCG1) expression. ABCG1 is crucial to pulmonary lipid homeostasis. ABCG1 deficiency results in lipid accumulation which promotes pro-inflammatory macrophage activation. Our results indicate that restoration of homeostatic ABCG1 levels by rosiglitazone correlates with both reduced pulmonary lipid accumulation, and decreased alveolar macrophage activation. These data confirm

and further support our previous observations that PPARγ pathways are critical in regulating MWCNT induced pulmonary granulomatous inflammation.

INTRODUCTION

Granulomatous lung diseases represent a significant health burden worldwide. Sarcoidosis is an inflammatory condition characterized by the presence of non-necrotizing granulomas which effects the lungs and mediastinal lymph nodes in 90% of clinical cases [23]. The etiology of sarcoidosis has not been determined, however current understanding suggest the presence of a poorly soluble antigen leading to an exuberant host immune response in genetically susceptible individuals [32]. Epidemiological studies have found a correlation between pulmonary sarcoidosis and exposure to wood-burning stoves, fireplaces and certain occupations such as firefighters [68;75;114]. An increased incidence of sarcoid-like granulomatous lesions have also been reported in first responders present at the September 2001 World Trade Center Disaster [65]. These environments have been shown to contain particulate matter of respirable sizes, including carbon nanotubes. Carbon nanotubes (CNT) are produced as byproducts of combustion or manufactured for a variety of commercial applications. Evaluation of the respiratory toxicology of these materials has found the potential to induce pulmonary granulomatous lesions in exposed animals [79;96]. These observations prompted our laboratory to investigate the use of multiwall carbon nanotubes (MWCNT) to generate a murine model of pulmonary granulomatous inflammation to study pulmonary sarcoidosis [58].

Previous methods utilized to induce pulmonary granulomas included the administration of pathogens or introduction of antigen bound sepharose beads into the tail vein of sensitized animals [33;63;76]. While these models have advanced our understanding of pulmonary granuloma formation they have notable drawbacks

including the presence of active pathogens, eliciting granuloma in the pulmonary capillaries instead of the airways and a relatively short resolution time. In our studies, evaluation of mice 60 days following MWCNT instillation found the persistence of granulomatous lesions throughout the lung [58]. Further studies demonstrated that the MWCNT model closely mimics sarcoidosis pathophysiology, including elevated expression of inflammatory mediators and reduced expression and activity of alveolar macrophage peroxisome proliferator-activated receptor gamma (PPARγ) [58;59;95].

PPARγ, a ligand-activated nuclear transcription factor, has been shown to limit pro-inflammatory macrophage activation [117]. PPARγ regulates gene expression by selectively binding PPARγ-response elements, promoting target gene expression, or through the inhibition of other transcription factors such as nuclear factor-κB (NF-κB) [47;115]. PPARγ, constitutively active in alveolar macrophages of healthy individuals, is deficient in multiple lung diseases including alveolar macrophages of pulmonary sarcoidosis patients [27;35;73]. The importance of alveolar macrophage PPARγ to pulmonary homeostasis is demonstrated by macrophage-specific PPARγ knockout mice. These animals exhibit increased Th-1 pro-inflammatory cytokine expression and dysregulated pulmonary lipid catabolism [7;88].

PPARγ maintains pulmonary lipid homeostasis through the expression of alveolar macrophage ATP-binding cassette lipid transporter-G1 (ABCG1) [6;7]. Following uptake by scavenger receptors, such as the PPARγ-regulated cluster of differentiation-36 (CD36), lipids are catabolized and effluxed to extracellular acceptors by ABCG1, and the complimentary lipid transporter ABCA1 [109]. Deficiency of ABCG1 or ABCA1

results in pulmonary lipid accumulation and elevated inflammatory mediators [8;19;74;143]. The inability to properly efflux cholesterol leads to increased sensitivity to extracellular inflammatory signaling in ABCA1/ABCG1 deficient macrophages [147]. Our recent studies in alveolar macrophages from sarcoidosis patients and MWCNT instilled mice observed decreased expression of both ABCG1 and ABCA1 [16]. The deficiency of these lipid transporters correlates with increased alveolar macrophage lipid accumulation in MWCNT instilled animals [16].

These observations suggest that downregulation of ABCG1 and ABCA1 may contribute to MWCNT induced inflammation. We hypothesized that increase of the PPARγ-ABCG1 pathway would limit alveolar macrophage activation and pulmonary granuloma formation. To address this hypothesis we utilized the PPARγ-specific agonist rosiglitazone to activate PPARγ pathways. Results shown here indicate that rosiglitazone attenuates MWCNT induced granulomatous inflammation.

MATERIALS AND METHODS

Animal care and treatment: Animal studies were conducted in accordance with the National Institutes of Health guide for the care and use of Laboratory animals and with approval from the East Carolina University Institutional Animal Care and Use Committee. C57BL/6J wild type mice were purchased from The Jackson Laboratory (Bar Harbor, ME). An equal number of age and sex matched controls were randomly assigned into experimental groups. Rosiglitazone laden diets were produced by Teklad Diets (Madison, MI), incorporating rosiglitazone (Cayman Chemical. Ann Arbor, MI) into standard rodent chow (Prolab RMH 300, LabDiet; St. Louis, MO), delivering 2, 6 or 12mg/kg/day (TD.160572, TD.160573 and TD.160574 respectively). Diets were administered daily, three days prior to instillation of multiwall carbon nanotubes (MWCNT) until necropsy at the indicated time point.

MWCNT Model: Pulmonary granulomas were generated by oropharyngeal aspiration of 100μg MWCNT (Cat.900-1501, Lot: GS1801) purchased from SES Research, Houston Texas as previously described [58]. Animals were euthanized with tribromoethanol and bronchoalveolar lavage (BAL) was performed for the collection of BAL cells as previously described [88]. Differential counts were performed on cytospins stained with modified Wright's stain. Histological analysis was performed on un-lavaged lungs inflated with formalin as previously described [58].

RNA purification and analysis: Total RNA was collected from BAL cell pellets with the miRNeasy Micro Kit and protocol (Qiagen. Valencia, CA). Primers were obtained from Qiagen for ATP binding cassette (ABC) transporter-A1 (Abca1, PPM03952F), Abcg1 (PPM03895A), chemokine (C-C motif) ligand-2 (Ccl2, PPM03151G),

Glyceraldehyde-3-phosphate-dehydrogenase (Gapdh, PPM02946E), peroxisome proliferator activated receptor-gamma (PPARγ, PPM05108B) and osteopontin (Spp1, PPM03648C). Relative gene expression of complimentary DNA synthesized with the RT2 First Strand Kit was evaluated on an ABI Prism 7300 system (Applied Biosystems. Foster City, CA) in comparison to Gapdh using the $2^{-\Delta\Delta CT}$ method [82].

Immunohistochemistry: BAL cytospins of freshly isolated BAL cells were fixed with 4% paraformaldehyde, permeabilized with 0.3% Triton-X-100 and stained for NF-κB 1:200 (catalog# 6956S. Cell Signaling. Danvers, MA) overnight at 4^0C followed by Alexa-conjugated goat anti mouse IgG 1:1000 (Invitrogen. Carlsbad, CA). Slides were counterstained with propidium iodide (Vector Laboratories. Burlingame, CA) to facilitate nuclear localization. Images were acquired on a LSM 700 confocal microscope (Zeiss. Oberkochen, Germany). Quantification of NF-κB nuclear localization was quantified using ZEN Blue software (Zeiss). Differential analysis of BAL cells revealed that alveolar macrophages constituted the majority of cells (93.4%-99.7%; n≥ 6) at either 10 or 20 days post treatment with no significant differences among BAL samples from control or treated groups.

Analysis of Bronchoalveolar Lavage Fluid: Total cholesterol was measured using the Amplex Red Cholesterol Assay kit (Thermo Fisher Scientific. Waltham, MA) according to manufacturer's instructions in the presence of cholesterol esterase. Cholesterol was normalized to protein content of BAL Fluid measured by BCA assay (Thermo Fisher Scientific).

Quantitative Analysis of Tissue: Digital images of whole lung cross sections stained with hematoxylin & eosin were acquired on an Aperio ScanScope (Aperio Technologies, Inc. Vista, CA). Analysis was performed blindly on randomized digital images, scanning the entire lung at 20X magnification for pulmonary granulomas. A granuloma was defined as a carbon aggregate completely surrounded by tissue and associated with three or more cell nuclei. Quantification of total stained lung area and carbon content were performed by the Translational Pathology Lab (University of North Carolina, Chapel Hill) using the Aperio deconvolution method as previously described [127]. The length (L) and width (W) of the tracheobronchal lymph node, identified based on Van den Broeck et al. [133], was used to determine lymph node volume using the formula $(LxW^2)\pi/6$.

Statistical Analysis: All data represent the mean of at least three individual experiments ±SEM unless otherwise indicated. Statistical analysis was performed using GraphPad Prizm software (San Diego, CA). Two-tailed student's t-tests were utilized for the comparison between groups. For all tests, $p<0.05$ was considered statistically significant.

RESULTS

PPARγ Agonist Regulates Alveolar Macrophage Gene Expression 10 days post MWCNT-Instillation

Our previous studies have shown deficiency of PPARγ, ABCA1 and ABCG1 in alveolar macrophages from both sarcoidosis patients and the 60 day MWCNT model [16;35;59]. The inflammatory mediators, chemokine (C-C motif) ligand-2 (CCL2) and osteopontin, were elevated in sarcoidosis granulomatous tissue and in the 60 day MWCNT model [15;59;103;108]. In the present study we evaluated gene expression of alveolar macrophages isolated 10 days following MWCNT instillation. PPARγ, ABCA1 and ABCG1 expression were significantly decreased in MWCNT instilled animals compared to those receiving vehicle (Figure 1A). As expected, the expression of CCL2 and osteopontin was upregulated in MWCNT instilled mice (Figure 1B). To determine the optimal dose of rosiglitazone required to increase alveolar macrophage ABCG1 expression and decrease the expression of pro-inflammatory mediators, rosiglitazone was administered at 2, 6 or 12mg/kg/day. The expression of alveolar macrophage ABCG1 was significantly increased in animals receiving 6 and 12mg/kg diet (Figure 1C). Evaluation of pro-inflammatory mediators found rosiglitazone capable of limiting CCL2 and osteopontin expression in a dose-dependent manner (Figure 1D,E). The optimal dose of rosiglitazone required to increase alveolar macrophage ABCG1 and limit pro-inflammatory mediator expression was 6mg/kg (Figure 1).

Histological examination of lung morphology confirmed our previous observation that granulomas at 10 days post-instillation were loosely formed [58]. Evaluation of the

frequency and severity of granulomatous inflammation using a previously described scoring system [59], found no difference between MWCNT instilled animals given rosiglitazone and normal chow (data not shown). To determine if the continuation of rosiglitazone would limit pulmonary granuloma formation, animals were evaluated 20 days post MWCNT instillation.

Rosiglitazone Inhibits MWCNT induced Pulmonary Granuloma Formation

Quantitative measurements were performed on digital images of lung tissue from MWCNT instilled mice receiving normal chow or the optimal dose of rosiglitazone (6mg/kg). The administration of rosiglitazone 20 days post-instillation: 1) significantly decreased the number of granulomas per lung area (Figure 2A); 2) limited the size of granulomatous lesions (Figure 2B); and 3) reduced the total carbon deposition in the lungs compared to animals receiving normal chow (Figure 2C). During gross dissection of the thoracic cavity, carbon deposition was noted in the cranial mediastinal lymph node. Quantification of lymph node volume revealed a significant increase following MWCNT instillation compared to mice receiving vehicle, and further lymphadenopathy in animals receiving rosiglitazone (Figure 2D). As a measure of total lung injury, protein concentration of the BAL fluid (BALF) was evaluated. MWCNT instillation resulted in significantly higher BALF protein concentration compared to animals receiving vehicle, while administration of rosiglitazone attenuated this increase (Figure 2E).

Rosiglitazone limits Alveolar Macrophage Activation and Pulmonary Dyslipidemia following MWCNT Instillation

Administration of rosiglitazone (6mg/kg) significantly attenuated the expression of alveolar macrophage CCL2 and osteopontin expression 20 days post MWCNT instillation (Figure 3B/C). We performed further studies to determine the mechanism by which rosiglitazone limited pro-inflammatory gene expression. PPARγ is capable of limiting pro-inflammatory gene expression through trans-repression of NF-κB activity [47;115]. Analysis of alveolar macrophages from MWCNT instilled mice demonstrated significantly less nuclear p65 localization in animals receiving rosiglitazone laden diet compared to controls (Figure 3A).

Decreased expression of alveolar macrophage PPARγ, ABCA1 and ABCG1 was also observed 20 days post MWCNT instillation (Figure 4A-C). Rosiglitazone did not affect the expression of PPARγ or ABCA1 (Figure 4A, B). In comparison, expression of alveolar macrophage ABCG1, a target gene of PPARγ, was significantly increased in MWCNT instilled mice receiving rosiglitazone compared to those receiving normal chow (Figure 4C). CD36 expression is slightly increased in MWCNT instilled animals, but was further up-regulated in animals receiving rosiglitazone (Figure 4D). To assess the rate of alveolar macrophage lipid catabolism we evaluated intracellular and extracellular lipids. Intracellular lipid accumulation was evaluated by determining mean alveolar macrophage diameter. Mice instilled with MWCNT had significantly larger alveolar macrophages compared to controls, while administration of rosiglitazone attenuated the

increase in cell size (Figure 4E). Total cholesterol accumulation in BAL fluid following MWCNT instillation was also reduced by administration of rosiglitazone (Figure 4F).

DISCUSSION

We have described a murine model of MWCNT induced granulomatous lung disease which closely mimics pulmonary sarcoidosis, including the deficiency of alveolar macrophage PPARγ. The ablation of alveolar macrophage PPARγ exacerbates MWCNT induced pulmonary granulomatous disease as well as pro-inflammatory alveolar macrophage activation [59]. Here we demonstrate that the PPARγ agonist rosiglitazone significantly limits alveolar macrophage activation, pulmonary granuloma formation and pulmonary lipid dysregulation following MWCNT instillation. These observations suggest that regulation of alveolar macrophage PPARγ may serve as a novel target for limiting pulmonary granulomatous inflammation.

Pretreatment with rosiglitazone limited the expression of pro-inflammatory mediators following MWCNT instillation. PPARγ can regulate inflammatory gene expression by trans-repression, the ability to interfere with the activity of other transcription factors such as NF-κB [47;115]. Alveolar macrophages of pulmonary sarcoidosis patients have significantly higher NF-κB activation compared to healthy individuals [35]. Our studies demonstrate that rosiglitazone inhibits NF-κB nuclear localization in MWCNT instilled animals. This observation is consistent with an inverse relationship between PPARγ and NF-κB activity. Additionally, CCL2 and osteopontin expression are regulated by NF-κB activity [89;148]. Interestingly, CCL2 or osteopontin-deficient mice develop less severe pulmonary granulomas in response to infectious stimuli [83;104]. These data suggest that such mediators may play a role in granuloma progression. The upregulation of these mediators in both human sarcoidosis and in

MWCNT instilled mice, beginning as early as ten days post instillation, also supports a critical role for these mediators in pulmonary granulomatous disease progression.

The frequency and severity of granulomatous lesions are attenuated by rosiglitazone 20 days post MWCNT instillation. The reduction of BAL fluid protein concentration in rosiglitazone treated animals also suggests attenuation of total lung injury. Previous reports have noted BAL fluid albumin concentration increased in a dose dependent manner following MWCNT instillation [112]. In addition to the decrease in frequency and severity of granulomas 20 days post-instillation, a decrease in pulmonary carbon content was also observed. Inhaled particulate matter has been shown to clear through pulmonary lymphatics [2;126]. The increase in mediastinal lymph node volume may suggest that carbon is cleared through this pathway when not incorporated into granuloma. Changes in mediastinal lymphadenopathy warrant further study with regard to carbon content and identity of lymph node cells.

In this report, we show the treatment with rosiglitazone significantly limits MWCNT induced pulmonary lipid accumulation. Our previous studies have shown alveolar macrophages of 60 day MWCNT instilled animals have increased intracellular lipid accumulation, a phenotype which promotes pro-inflammatory signaling in ABC-lipid transporter deficient macrophages [16;147]. Our data suggest that rosiglitazone increases alveolar macrophage lipid catabolism by promoting uptake and export, by the PPARγ target genes CD36 and ABCG1. The slight increase of CD36 expression observed in alveolar macrophages of MWCNT instilled animals may be attributed to increased intracellular lipid content. Oxidized lipids have been shown to promote CD36 expression in a PPARγ-independent mechanism [36]. These observations suggest that

pulmonary lipid dysregulation following exposure to MWCNT may contribute to alveolar macrophage pro-inflammatory activation.

The current findings support and confirm our previous study examining the role of PPARγ deficiency in granulomatous disease [59]. Whereas PPARγ deficiency exacerbates granulomatous disease, ligand-dependent induction of PPARγ activity exerts a protective effect and constrains granuloma size. These data also strongly suggest that the PPARγ pathway responsible for the protective effect is the regulation via target gene activity, of intracellular pro-inflammatory lipid accumulation.

Figure 1: Rosiglitazone Regulates Alveolar Macrophage Gene Expression 10 days following MWCNT instillation. Quantitative-PCR analysis of the lipid regulatory genes (A) peroxisome proliferator activated receptor-γ (PPARγ), ATP-binding cassette lipid transporter-G1 (ABCG1), and ABCA1; and inflammatory mediators (B) CCL2 and osteopontin (OPN) in BAL cells of vehicle or MWCNT instilled mice. Effect of rosiglitazone dose curve on alveolar macrophage (C) ABCG1, (D) CCL2 and (E) osteopontin expression. ★$p<0.05$, $n \geq 3$/treatment.

Figure 1

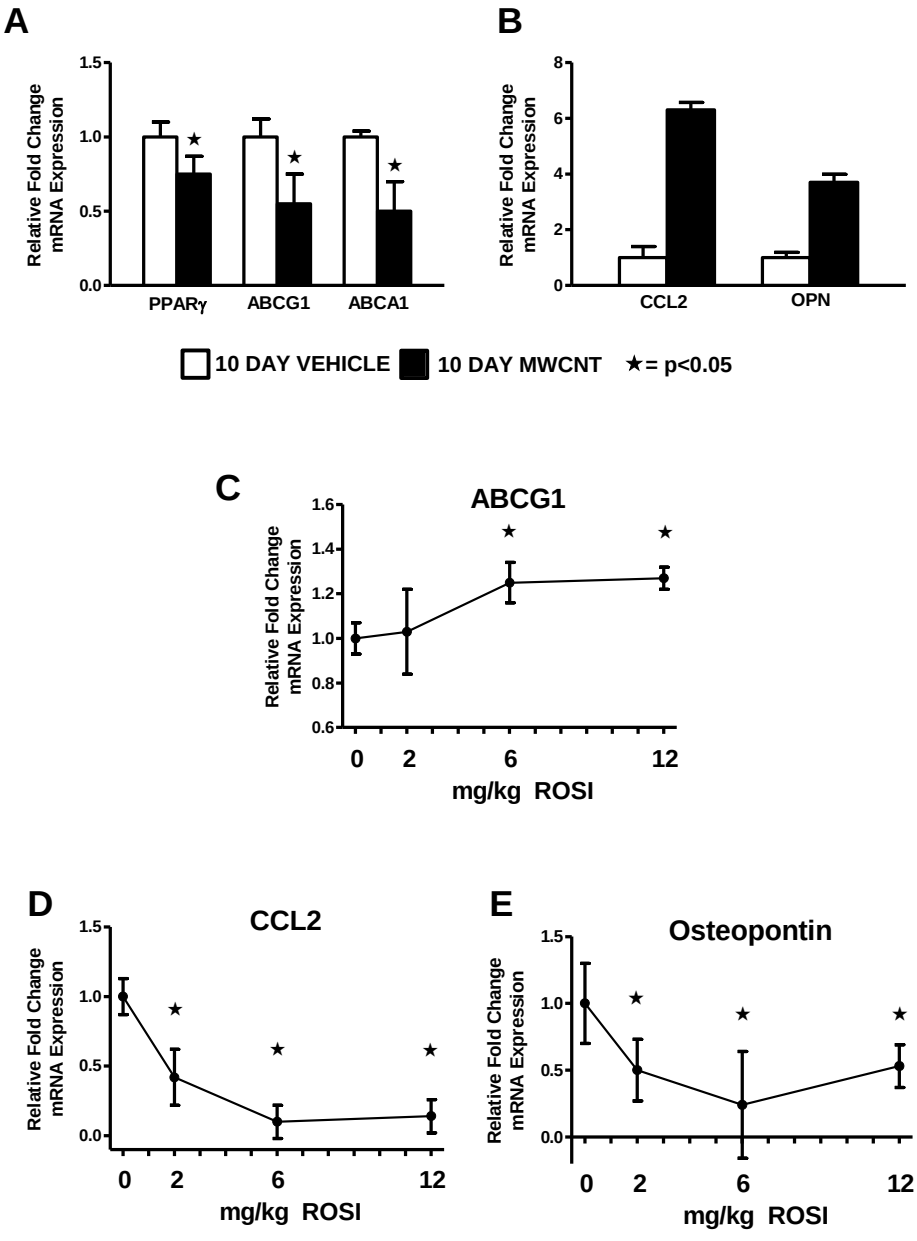
A
B
Relative Fold Change mRNA Expression
1.5
1.0
0.5
0.0
PPARγ
ABCG1
ABCA1
8
6
4
2
0
CCL2
OPN
10 DAY VEHICLE
10 DAY MWCNT
★= p<0.05
C
ABCG1
1.6
1.4
1.2
1.0
0.8
0.6
0
2
6
12
mg/kg ROSI
D
CCL2
E
Osteopontin

Figure 2: Rosiglitazone Inhibits Pulmonary Granuloma Formation 20 days post MWCNT Instillation. Quantitative analysis of H&E stained lung tissue was utilized to evaluate (A) the average number of granulomas, (B) average granuloma size, (C) and total carbon deposition in MWCNT instilled animals receiving normal chow or rosiglitazone (6mg/kg). Evaluation of (D) mediastinal lymph node volume and (E) BAL-fluid protein concentration in vehicle and MWCNT instilled animals receiving normal chow or rosiglitazone (6mg/kg). ★$p<0.05$, $n\geq5$/treatment.

Figure 2

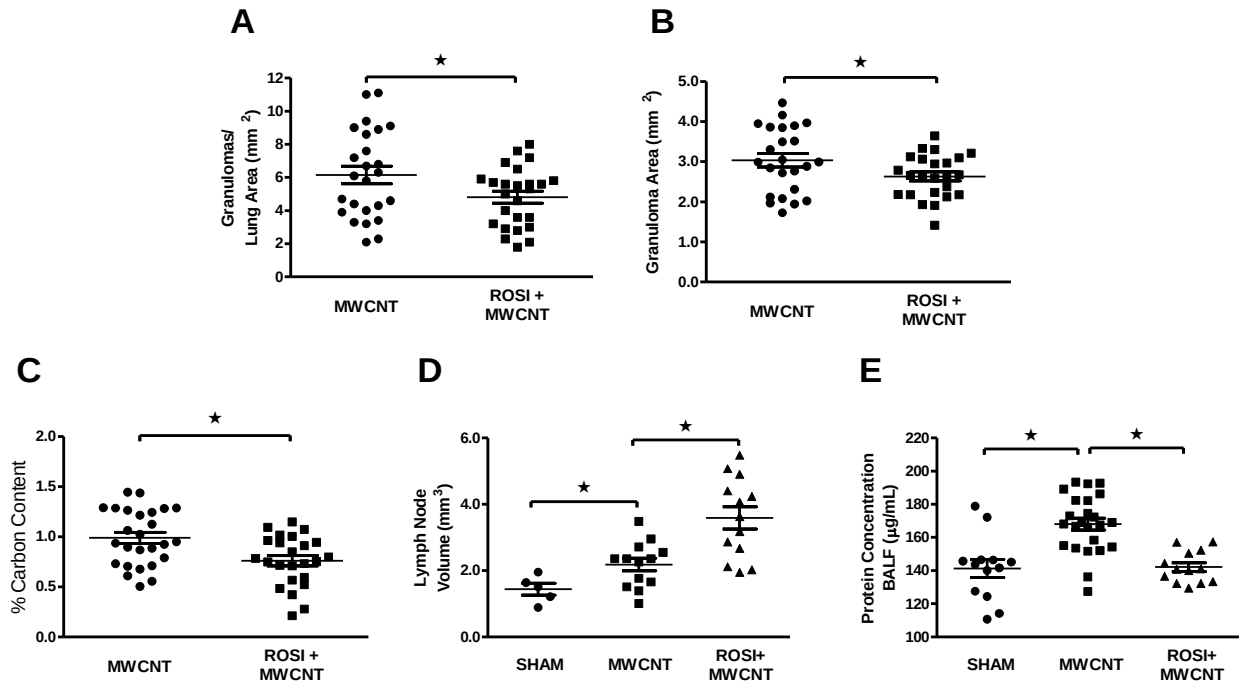
A
Granulomas/ Lung Area (mm 2)
12
10
8
6
4
2
0
MWCNT
ROSI + MWCNT
B
Granuloma Area (mm 2)
5.0
4.0
3.0
2.0
1.0
0.0
MWCNT
ROSI + MWCNT
C
% Carbon Content
2.0
1.5
1.0
0.5
0.0
MWCNT
ROSI + MWCNT
D
Lymph Node Volume (mm3)
6.0
4.0
2.0
0.0
SHAM
MWCNT
ROSI+ MWCNT
E
Protein Concentration BALF (µg/mL)
220
200
180
160
140
120
100
SHAM
MWCNT
ROSI+ MWCNT

Figure 3: Rosiglitazone Reduces Alveolar Macrophage Activation 20 days post MWCNT Instillation. (A) Mean fluorescence intensity of nuclear NF-κB p65 protein in MWCNT instilled animals receiving normal chow or rosiglitazone (6mg/kg), ≤99cells/animal. Quantitative-PCR analysis of (B) CCL2 and (C) osteopontin expression in BAL cells of vehicle or MWCNT instilled animals receiving normal chow or rosiglitazone (6mg/kg). ★$p<0.01$, $n\geq5$/treatment.

Figure 3:

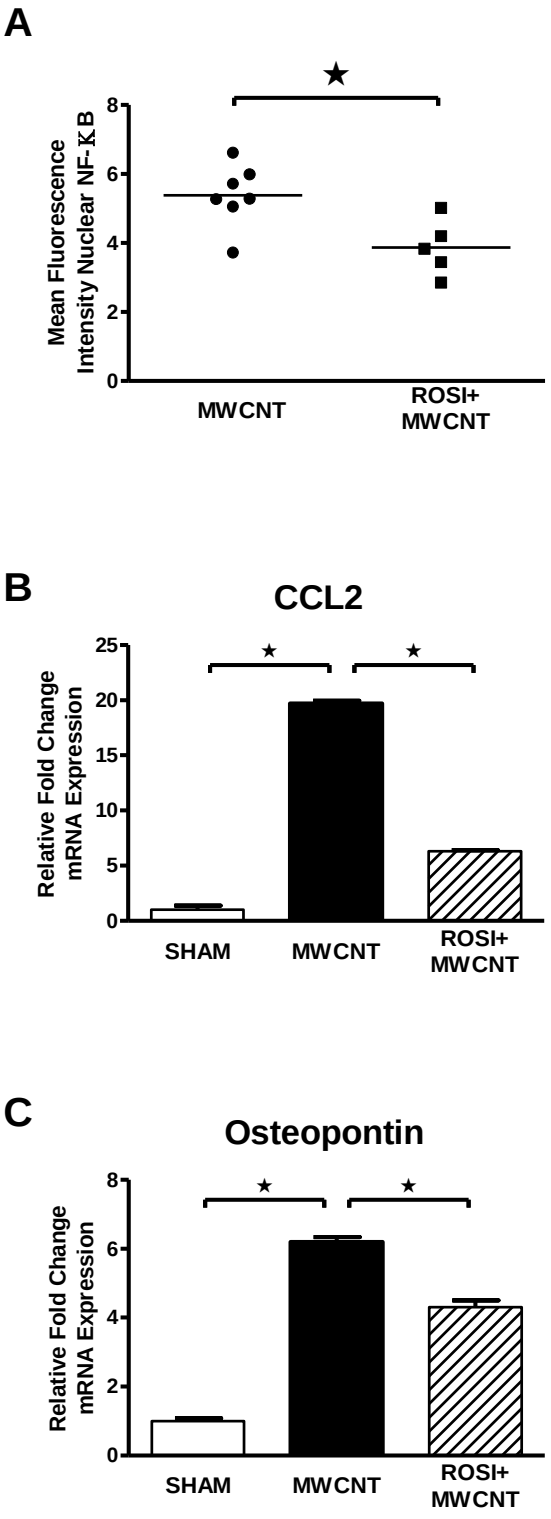
A
Mean Fluorescence Intensity Nuclear NF-ΚB
0
2
4
6
8
MWCNT
ROSI+ MWCNT
B
CCL2
Relative Fold Change mRNA Expression
0
5
10
15
20
25
SHAM
MWCNT
ROSI+ MWCNT
C
Osteopontin
Relative Fold Change mRNA Expression
0
2
4
6
8
SHAM
MWCNT
ROSI+ MWCNT

Figure 4: Rosiglitazone limits pulmonary dyslipidemia 20 days following MWCNT instillation. Quantitative-PCR analysis of the lipid regulatory genes (A) PPARγ (B) ABCA1, (C) ABCG1 and (D) CD36 in vehicle or MWCNT instilled animals receiving normal chow or rosiglitazone (6mg/kg). Evaluation of (E) mean alveolar macrophage diameter and (E) total cholesterol content of BAL fluid of vehicle and MWCNT instilled mice receiving normal chow or rosiglitazone (6mg/kg). ★$p<0.01$, $n\geq5$/treatment.

Figure 4:

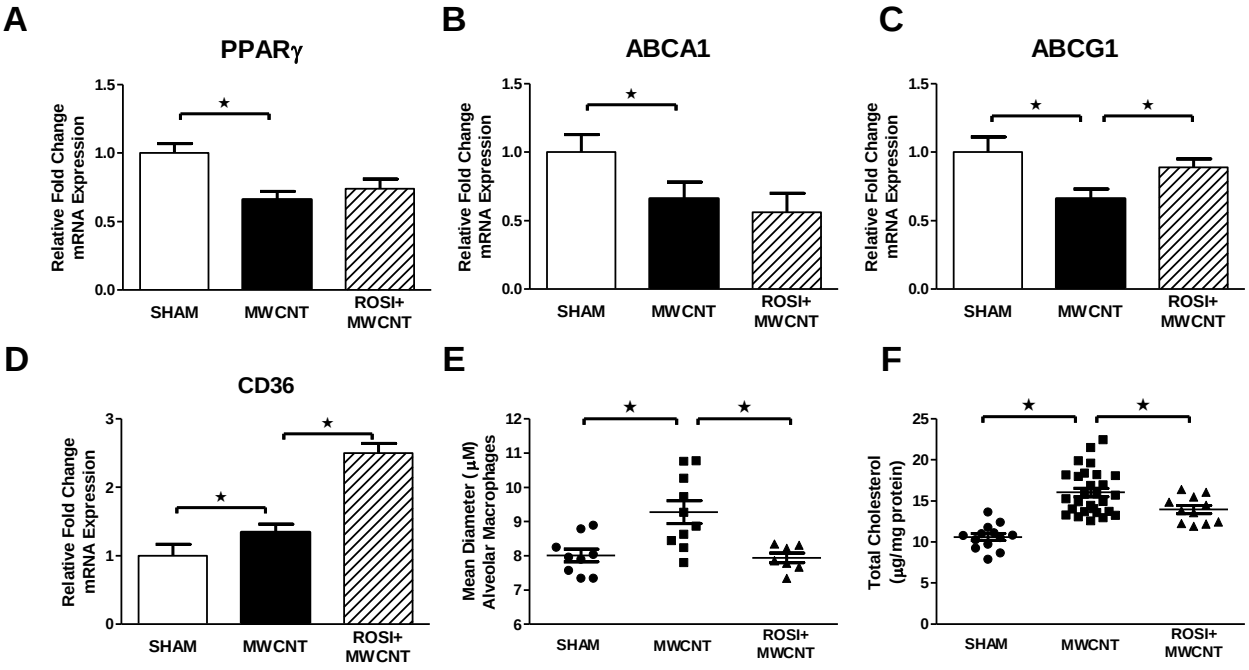
A
PPARγ
Relative Fold Change mRNA Expression
1.5
1.0
0.5
0.0
SHAM
MWCNT
ROSI+ MWCNT
B
ABCA1
Relative Fold Change mRNA Expression
1.5
1.0
0.5
0.0
SHAM
MWCNT
ROSI+ MWCNT
C
ABCG1
Relative Fold Change mRNA Expression
1.5
1.0
0.5
0.0
SHAM
MWCNT
ROSI+ MWCNT
D
CD36
Relative Fold Change mRNA Expression
3
2
1
0
SHAM
MWCNT
ROSI+ MWCNT
E
Mean Diameter (μM) Alveolar Macrophages
12
11
10
9
8
7
6
SHAM
MWCNT
ROSI+ MWCNT
F
Total Cholesterol (μg/mg protein)
25
20
15
10
5
0
SHAM
MWCNT
ROSI+ MWCNT

ACKNOWLEDGEMENTS: This work was supported by the National Institutes of Health grants ES022462 and ES025191 awarded to M.J.T. and by P30-ES025128.

The work presented in this chapter was successfully published:

M. McPeek, A. Malur, D.A. Tokarz, G. Murray, B.P. Barna, M.J. Thomassen, PPAR-gamma pathways attenuate pulmonary granuloma formation in a carbon nanotube induced murine model of sarcoidosis. *Biochem.Biophys.Res.Commun*. 2018; 503:684-690.

CHAPTER FIVE

GENERAL DISCUSSION AND FUTURE DIRECTIONS

Our laboratory has described a murine model of chronic granulomatous inflammation elicited by multiwall carbon nanotubes which bears striking similarity to pulmonary sarcoidosis. Alveolar macrophages of sarcoidosis patients and MWCNT instilled mice demonstrate 1) decreased expression and activity of PPARγ, 2) decreased expression of the lipid transporters ABCA1 and ABCG1 and 3) increased expression of the pro-inflammatory mediators CCL2 and osteopontin. Further investigation found that macrophage-specific deficiency of PPARγ promotes MWCNT induced granuloma formation, inflammation and fibrosis [59;86]. These studies aimed to further determine how these factors contributed to pulmonary granuloma formation and inflammation. We hypothesized that the deficiency of the PPARγ-ABCG1 pathway and subsequent pulmonary lipidosis promote MWCNT induced granuloma formation.

Here we demonstrate that the deficiency of ATP binding cassette lipid transporter ABCG1, but not ABCA1, promotes pulmonary granuloma formation, pulmonary fibrosis, pro-fibrotic mediators and the expression of CCL2 and osteopontin. We further demonstrate the administration of the PPARγ specific agonist rosiglitazone increased the expression of alveolar macrophage ABCG1, reduced pulmonary lipid accumulation and limits the formation of pulmonary granulomas and the expression of the pro-inflammatory mediators CCL2 and osteopontin. The data presented here demonstrate the deficiency of alveolar macrophage ABCG1 is not only an effect of, but actively promotes pulmonary inflammation and injury. These studies also support our hypothesis that dysregulation of pulmonary lipid homeostasis may directly influence pulmonary granuloma formation.

Several questions arise from the work reported in this dissertation. An unexpected difference found during this study was PPARγ mRNA expression. Significantly downregulated in wild-type alveolar macrophages, PPARγ mRNA expression in ABC-lipid transporter knockout animals demonstrate a slight but nonsignificant decrease compared to wild-type mice and was not affected by MWCNT instillation. Further studies will be required to evaluate the activity of PPARγ nuclear activity in these cells. Preliminary observations suggest the ABCG1-KO and ABCA1/ABCG1-DKO models exhibit increased lipid accumulation and general pulmonary inflammation compared to PPARγ-KO mice. Paradoxically, the MWCNT induced granulomas in PPARγ-KO mice are more concentric and well organized compared to the irregular borders and multiple carbon aggregates observed in ABCG1-KO and ABCA1/ABCG1-KO mice. This observations may suggest the lung environment is more dynamic in ABCG1 deficient animals. Previous studies have indicated ABCG1 deficiency promotes leukocyte infiltration into the airways and lung interstitium [40;143]. Visual observation of ABCG1-KO animals following MWCNT instillation also noted increased bronchial associated lymphoid tissue and lymphoid aggregates throughout the lung compared to wild-type animals. Characterization of the infiltrating leukocytes in the airways and pulmonary interstitium may lead to a better understanding of how the pulmonary granuloma is formed and maintained.

Another area of interest is the identification of specific mechanisms regulating pulmonary lipid accumulation and inflammation. Macrophage lipid accumulation has been shown to increase the sensitivity of these cells to pro-inflammatory ligands. Increased cholesterol content of the plasma membrane promotes the formation of lipid-

rafts, which organize cell signaling molecules such as toll-like receptors [74;147]. Toll like receptors recognize pathogens and endogenous damage associated molecular patterns which enhance the inflammatory response [69]. The role of these receptors have also been investigated in the pathology of sarcoidosis. Genetic association studies have identified the TLR4 and TLR9 genes with development of sarcoidosis [122;123]. Further studies demonstrated bronchoalveolar lavage (BAL) cells of sarcoidosis patients' exhibit increase cytokine production in response to TLR2 ligands and have significantly higher TLR9 mRNA expression and alveolar macrophage protein content compared to controls individuals [44;121]. Interestingly, TLR4 ligands have been shown to inhibit PPARγ mRNA expression in an NF-κB dependent mechanism [100].

In addition to promoting toll-like receptor signaling, dysregulation of cholesterol homeostasis has been found to activate the NLRP3 inflammasome [42]. The inflammasome is a multimeric protein complex which proteolytically activates interleukin-1β (IL-1β) [38]. Evaluation of alveolar macrophages from a large cohort of sarcoidosis patients found a significant increase in NLRP3 mRNA expression and reduced granuloma formation in a NLRP3 deficient murine model [113]. The inflammasome has also been implicated in promoting MWCNT induced acute inflammation and induction of pro-fibrotic mediators [48;60]. During the course of our studies, we observed the administration of rosiglitazone limits MWCNT induced IL-1β expression 20 days following MWCNT instillation.

Changes in lipid homeostasis have also been implicated in the regulation of the adaptive immune response [42;138]. Deficiency of ABCG1 has been found to promote lymphocyte infiltration and the production of autoantibodies against oxidized lipid

species of the lung [9;143]. In sarcoidosis, activated T-cells propagate the inflammatory process [51]. Elevated CD4/CD8 ratio is commonly associated with pulmonary sarcoidosis and has been established as a strong diagnostic indicator of the disease [137;142]. Our studies found the deficiency of macrophage ABCG1 promotes MWCNT induced mediastinal lymphadenopathy, suggesting an effect on adaptive immune programs. Increasing our understanding of these interactions may lead to improved therapies.

Currently there are limited treatment options available for pulmonary sarcoidosis, those include corticosteroids, immunosuppressive agents and biologics. Corticosteroids have been shown to be modestly effective and are commonly the initial treatment option in patients who do not undergo spontaneous remission [21;62;111]. However there are significant side effects associated with these agents, particularly when used for extended periods of time [21]. Immunosuppressive agents have also been utilized during steroid-sparing periods and for individuals who do not tolerate steroids well [22]. More recently the use of biologics have been evaluated. The use of TNFα (tumor necrosis factor-α) inhibitors such as Infliximab or Thalidomide, which limits TNFα release from alveolar macrophages have been shown to be effective in refractory sarcoidosis [21]. Given these observations other clinical options may improve the clinical outcomes of sarcoidosis.

Recent studies have indicated cholesterol regulatory genes may serve as novel pharmacological targets in the treatment of lung disease. The subject of a recent comprehensive review [50], cholesterol targeting agents have been utilized in experimental models of asthma, acute lung injury, COPD and pulmonary fibrosis. A

recent clinical trial (NCT00279708) has evaluated the use of the cholesterol targeting agent atorvastatin to extend the amount of time pulmonary sarcoidosis patients were taken off or given reduced doses of corticosteroids. Individuals randomized into the control group averaged 257 days until steroids were resumed while those individuals receiving Atorvastatin averaged 301 days, however no statistical data or follow up outcome measures have been provided. In addition to regulating hepatic lipid synthesis, statins are known to have anti-inflammatory properties through inhibition of NFκB but also promote the activity of PPARγ [66]. These observation prompt the question, could a similar retrospective study be conducted evaluating patients receiving a direct PPARγ agonist such as rosiglitazone or another thiazolidinedione?

The work presented here addresses the role of PPARγ, ABCG1 and lipid accumulation in granulomatous lung disease. We hypothesized that the PPARγ-ABCG1 pathway and pulmonary lipid accumulation would exacerbate granulomatous inflammation. These data indicate there is a unique relationship between pulmonary lipid homeostasis and inflammatory lung disease and understanding this relationship will contribute to the development of novel therapies for inhibiting inflammation in response to environmental antigens or in the case of chronic granulomatous lung diseases.

REFERENCES

[1] C. Agostini, A. Meneghin, G. Semenzato, T-lymphocytes and cytokines in sarcoidosis. Curr.Opin.Pulm.Med. 8 (2002) 435-440.

[2] S. Aiso, H. Kubota, Y. Umeda, T. Kasai, M. Takaya, K. Yamazaki, K. Nagano, T. Sakai, S. Koda, S. Fukushima, Translocation of intratracheally instilled multiwall carbon nanotubes to lung-associated lymph nodes in rats. Ind.Health 49 (2011) 215-220.

[3] H.M. Algood, P.L. Lin, J.L. Flynn, Tumor necrosis factor and chemokine interactions in the formation and maintenance of granulomas in tuberculosis. Clin.Infect.Dis. 41 Suppl 3 (2005) S189-S193.

[4] S. Ameshima, H. Golpon, C.D. Cool, D. Chan, R.W. Vandivier, S.J. Gardai, M. Wick, R.A. Nemenoff, M.W. Geraci, N.F. Voelkel, Peroxisome proliferator-activatd receptor gamma (PPARg) expression is decreased in pulmonary hypertension and affects endothelial cell growth. Cir.Res. 92 (2003) 1162-1169.

[5] A. Azuma, Y.J. Li, S. Abe, J. Usuki, K. Matsuda, S. Henmi, Y. Miyauchi, K. Ueda, A. Izawa, S. Sone, S. Hashimoto, S. Kudoh, Interferon-{beta} inhibits bleomycin-induced lung fibrosis by decreasing transforming growth factor-{beta} and thrombospondin. Am.J.Respir.Cell Mol.Biol. 32 (2005) 93-98.

[6] A.D. Baker, A. Malur, B.P. Barna, M.S. Kavuru, A.G. Malur, M.J. Thomassen, PPARgamma regulates the expression of cholesterol metabolism genes in alveolar macrophages. Biochem.Biophys.Res.Commun. 393 (2010) 682-687.

[7] A.D. Baker, A. Malur, B.P. Barna, S. Ghosh, M.S. Kavuru, A.G. Malur, M.J. Thomassen, Targeted PPAR{gamma} deficiency in alveolar macrophages disrupts surfactant catabolism. J.Lipid Res. 51 (2010) 1325-1331.

[8] A. Baldan, A.V. Gomes, P. Ping, P.A. Edwards, Loss of ABCG1 results in chronic pulmonary inflammation. J Immunol 180 (2008) 3560-3568.

[9] A. Baldan, A. Gonen, C. Choung, X. Que, T.J. Marquart, I. Hernandez, I. Bjorkhem, D.A. Ford, J.L. Witztum, E.J. Tarling, ABCG1 is required for pulmonary B-1 B cell and natural antibody homeostasis. J.Immunol. 193 (2014) 5637-5648.

[10] A. Baldan, P. Tarr, R. Lee, P.A. Edwards, ATP-binding cassette transporter G1 and lipid homeostasis. Curr.Opin.Lipidol. 17 (2006) 227-232.

[11] A. Baldan, P. Tarr, C.S. Vales, J. Frank, T.K. Shimotake, S. Hawgood, P.A. Edwards, Deletion of the Transmembrane Transporter ABCG1 Results in Progressive Pulmonary Lipidosis. J.Biol.Chem. 281 (2006) 29401-29410.

[12] J.J. Bang, P.A. Guerrero, D.A. Lopez, L.E. Murr, E.V. Esquivel, Carbon nanotubes and other fullerene nanocrystals in domestic propane and natural gas combustion streams. J.Nanosci.Nanotechnol. 4 (2004) 716-718.

[13] B.P. Barna, M.A. Judson, M.J. Thomassen. Carbon Nanotubes and Chronic Granulomatous Disease. Nanomaterials 4, 508-521. 2014.
Ref Type: Journal (Full)

[14] B.P. Barna, D.A. Culver, S. Abraham, A. Malur, T.L. Bonfield, N. John, C.F. Farver, J.A. Drazba, B. Raychaudhuri, M.S. Kavuru, M.J. Thomassen, Depressed peroxisome proliferator-activated receptor gamma (PPARgamma) is indicative of severe pulmonary sarcoidosis: possible involvement of interferon gamma (IFN-gamma). Sarcoidosis.Vasc.Diffuse.Lung Dis. 23 (2006) 93-100.

[15] B.P. Barna, I. Huizar, A. Malur, M. McPeek, I. Marshall, M. Jacob, L. Dobbs, M.S. Kavuru, M.J. Thomassen, Carbon nanotube-induced pulmonary granulomatous disease: twist1 and alveolar macrophage m1 activation. Int.J Mol.Sci 14 (2013) 23858-23871.

[16] B.P. Barna, M. McPeek, A. Malur, M.B. Fessler, C.J. Wingard, L. Dobbs, K.M. Verbanac, M. Bowling, M.A. Judson, M.J. Thomassen, Elevated MicroRNA-33 in Sarcoidosis and a Carbon Nanotube Model of Chronic Granulomatous Disease. Am.J.Respir.Cell Mol.Biol. 54 (2016) 865-871.

[17] C. Basset-Leobon, L. Lacoste-Collin, J. Aziza, J.C. Bes, S. Jozan, M. Courtade-Saidi, Cut-off values and significance of Oil Red O-positive cells in bronchoalveolar lavage fluid. Cytopathology 21 (2010) 245-250.

[18] S.R. Bates, J.Q. Tao, K.J. Yu, Z. Borok, E.D. Crandall, H.L. Collins, G.H. Rothblat, Expression and biological activity of ABCA1 in alveolar epithelial cells. Am.J.Respir.Cell Mol.Biol. 38 (2008) 283-292.

[19] S.R. Bates, J.Q. Tao, H.L. Collins, O.L. Francone, G.H. Rothblat, Pulmonary abnormalities due to ABCA1 deficiency in mice. Am J Physiol Lung Cell Mol Physiol 289 (2005) L980-L989.

[20] R.P. Baughman, D.A. Culver, M.A. Judson, A concise review of pulmonary sarcoidosis. Am.J.Respir.Crit Care Med. 183 (2011) 573-581.

[21] R.P. Baughman, J.C. Grutters, New treatment strategies for pulmonary sarcoidosis: antimetabolites, biological drugs, and other treatment approaches. Lancet Respir.Med 3 (2015) 813-822.

[22] R.P. Baughman, H. Nunes, Therapy for sarcoidosis: evidence-based recommendations. Expert.Rev.Clin.Immunol. 8 (2012) 95-103.

[23] R.P. Baughman, A.S. Teirstein, M.A. Judson, M.D. Rossman, H. Yeager, E.A. Bresnitz, L. DePalo, G. Hunninghake, M.C. Iannuzzi, C.J. Johns, G. McLennan,

D.R. Moller, L.S. Newman, D.L. Rabin, C. Rose, B. Rybicki, S.E. Weinberger, M.L. Terrin, G.L. Knatterud, R. Cherniak, Clinical characteristics of patients in a case control study of sarcoidosis. Am.J.Respir.Crit.Care Med. 164 (2001) 1885-1889.

[24] R.P. Baughman, D.B. Winget, E.H. Bowen, E.E. Lower, Predicting respiratory failure in sarcoidosis patients. Sarcoidosis.Vasc.Diffuse.Lung Dis. 14 (1997) 154-158.

[25] R.P. Baughman, E.E. Lower, R.M. du Bois, Sarcoidosis. The Lancet 361 (2003) 1111-1118.

[26] A.E. Bochem, F.M. van der Valk, S. Tolani, E.S. Stroes, M. Westerterp, A.R. Tall, Increased Systemic and Plaque Inflammation in ABCA1 Mutation Carriers With Attenuation by Statins. Arterioscler.Thromb.Vasc.Biol. 35 (2015) 1663-1669.

[27] T.L. Bonfield, C.F. Farver, B.P. Barna, A. Malur, S. Abraham, B. Raychaudhuri, M.S. Kavuru, M.J. Thomassen, Peroxisome proliferator-activated receptor-gamma is deficient in alveolar macrophages from patients with alveolar proteinosis. Am.J.Respir.Cell Mol.Biol. 29 (2003) 677-682.

[28] A.E. Bortnick, E. Favari, J.Q. Tao, O.L. Francone, M. Reilly, Y. Zhang, G.H. Rothblat, S.R. Bates, Identification and characterization of rodent ABCA1 in isolated type II pneumocytes. Am J Physiol Lung Cell Mol Physiol 285 (2003) L869-L878.

[29] S.T. Brown, I. Brett, P.L. Almenoff, M. Lesser, M. Terrin, A.S. Teirstein, Recovery of cell wall-deficient organisms from blood does not distinguish between patients with sarcoidosis and control subjects. Chest 123 (2003) 413-417.

[30] A.B. Chai, A.J. Ammit, I.C. Gelissen, Examining the role of ABC lipid transporters in pulmonary lipid homeostasis and inflammation. Respir.Res. 18 (2017) 41.

[31] A. Chawla, Y. Barak, L. Nagy, D. Liao, P. Tontonoz, R.M. Evans, PPAR-g dependent and independent effects on macrophage-gene expression in lipid metabolism and inflammation. Nat.Med. 7 (2001) 48-52.

[32] E.S. Chen, D.R. Moller, Etiology of sarcoidosis. Clin Chest Med 29 (2008) 365-77, vii.

[33] S.W. Chensue, I.G. Otterness, G.I. Higashi, C.S. Forsch, S.L. Kunkel, Monokine production by hypersensitivity (Schistosoma mansoni egg) and foreign body (Sephadex bead)-type granuloma macrophages. Evidence for sequential production of IL-1 and tumor necrosis factor. J Immunol 142 (1989) 1281-1286.

[34] L.E. Crowley, R. Herbert, J.M. Moline, S. Wallenstein, G. Shukla, C. Schechter, G.S. Skloot, I. Udasin, B.J. Luft, D. Harrison, M. Shapiro, K. Wong, H.S. Sacks,

P.J. Landrigan, A.S. Teirstein, "Sarcoid like" granulomatous pulmonary disease in World Trade Center disaster responders. Am J Ind.Med 54 (2011) 175-184.

[35] D.A. Culver, B.P. Barna, B. Raychaudhuri, T.L. Bonfield, S. Abraham, A. Malur, C.F. Farver, M.S. Kavuru, M.J. Thomassen, Peroxisome proliferator-activated receptor gamma activity is deficient in alveolar macrophages in pulmonary sarcoidosis. Am.J.Respir.Cell Mol.Biol. 30 (2004) 1-5.

[36] M. D'Archivio, B. Scazzocchio, C. Filesi, R. Vari, M.T. Maggiorella, L. Sernicola, C. Santangelo, C. Giovannini, R. Masella, Oxidised LDL up-regulate CD36 expression by the Nrf2 pathway in 3T3-L1 preadipocytes. FEBS Lett. 582 (2008) 2291-2298.

[37] M.F. De Volder, S.H. Tawfick, R.H. Baughman, A.J. Hart, Carbon nanotubes: present and future commercial applications. Science 339 (2013) 535-539.

[38] N.D. De, C.M. De Nardo, E. Latz, New insights into mechanisms controlling the NLRP3 inflammasome and its role in lung disease. Am J Pathol. 184 (2014) 42-54.

[39] M. Dean, Y. Hamon, G. Chimini, The human ATP-binding cassette (ABC) transporter superfamily. J.Lipid Res. 42 (2001) 1007-1017.

[40] D.W. Draper, K.M. Gowdy, J.H. Madenspacher, R.H. Wilson, G.S. Whitehead, H. Nakano, A.R. Pandiri, J.F. Foley, A.T. Remaley, D.N. Cook, M.B. Fessler, ATP binding cassette transporter G1 deletion induces IL-17-dependent dysregulation of pulmonary adaptive immunity. J.Immunol. 188 (2012) 5327-5336.

[41] K.H. Ely, T. Cookenham, A.D. Roberts, D.L. Woodland, Memory T cell populations in the lung airways are maintained by continual recruitment. J.Immunol. 176 (2006) 537-543.

[42] M.B. Fessler, The Intracellular Cholesterol Landscape: Dynamic Integrator of the Immune Response. Trends Immunol. 37 (2016) 819-830.

[43] M.G. Foreman, D.M. Mannino, L. Kamugisha, G.E. Westney, Hospitalization for patients with sarcoidosis: 1979-2000. Sarcoidosis.Vasc.Diffuse.Lung Dis. 23 (2006) 124-129.

[44] M.I. Gabrilovich, J. Walrath, L.J. van, D. Nethery, M. Seifu, J.A. Kern, C.V. Harding, L. Tuscano, H. Lee, S.D. Williams, W. Mackay, J.F. Tomashefski, Jr., R.F. Silver, Disordered Toll-like receptor 2 responses in the pathogenesis of pulmonary sarcoidosis. Clin.Exp.Immunol. 173 (2013) 512-522.

[45] I.C. Gelissen, M. Harris, K.A. Rye, C. Quinn, A.J. Brown, M. Kockx, S. Cartland, M. Packianathan, L. Kritharides, W. Jessup, ABCA1 and ABCG1 synergize to mediate cholesterol export to apoA-I. Arterioscler.Thromb.Vasc.Biol 26 (2006) 534-540.

[46] A.K. Gerke, M. Yang, F. Tang, J.E. Cavanaugh, P.M. Polgreen, Increased hospitalizations among sarcoidosis patients from 1998 to 2008: a population-based cohort study. BMC.Pulm.Med. 12 (2012) 19.

[47] S. Ghisletti, W. Huang, S. Ogawa, G. Pascual, M.E. Lin, T.M. Willson, M.G. Rosenfeld, C.K. Glass, Parallel SUMOylation-dependent pathways mediate gene- and signal-specific transrepression by LXRs and PPARgamma. Mol.Cell 25 (2007) 57-70.

[48] T.A. Girtsman, C.A. Beamer, N. Wu, M. Buford, A. Holian, IL-1R signalling is critical for regulation of multi-walled carbon nanotubes-induced acute lung inflammation in C57Bl/6 mice. Nanotoxicology. 8 (2014) 17-27.

[49] C.K. Glass, K. Saijo, Nuclear receptor transrepression pathways that regulate inflammation in macrophages and T cells. Nat Rev Immunol 10 (2010) 365-376.

[50] K.M. Gowdy, M.B. Fessler, Emerging roles for cholesterol and lipoproteins in lung disease. Pulm.Pharmacol.Ther. 26 (2013) 430-437.

[51] J. Grunewald, A. Eklund, Role of CD4+ T cells in sarcoidosis. Proc.Am.Thorac.Soc. 4 (2007) 461-464.

[52] D. Gupta, R. Agarwal, A.N. Aggarwal, S.K. Jindal, Molecular evidence for the role of mycobacteria in sarcoidosis: a meta-analysis. Eur.Respir.J. 30 (2007) 508-516.

[53] S. Han, R.K. Mallampalli, The Role of Surfactant in Lung Disease and Host Defense against Pulmonary Infections. Ann.Am.Thorac.Soc.2015).

[54] D. Hayes, Jr., S. Kirkby, S. McCoy, H.M. Mansour, M. Khosravi, H. Strawbridge, J.D. Tobias, Reduction of lipid-laden macrophage index after laparoscopic Nissen fundoplication in cystic fibrosis patients after lung transplantation. Clin.Transplant. 27 (2013) 121-125.

[55] J.R. Hoidal, D. Schmeling, P.K. Peterson, Phagocytosis, bacterial killing, and metabolism by purified human lung phagocytes. J.Infect.Dis. 144 (1981) 61-71.

[56] J.F. Holter, H.K. Park, K.W. Sjoerdsma, Y.P. Kataria, Nonviable Autologous Bronchoalveolar Lavage Cell Preparations Induce Intradermal Epithelioid Cell Granulomas in Sarcoidosis Patients. Am.Rev.Respir Dis. 148 (1983) 844-871.

[57] R.H. Hubner, W. Gitter, N.E. El Mokhtari, M. Mathiak, M. Both, H. Bolte, S. Freitag-Wolf, B. Bewig, Standardized quantification of pulmonary fibrosis in histological samples. Biotechniques 44 (2008) 507.

[58] I. Huizar, A. Malur, Y.A. Midgette, C. Kukoly, P. Chen, P.C. Ke, R. Podila, A.M. Rao, C.J. Wingard, L. Dobbs, B.P. Barna, M.S. Kavuru, M.J. Thomassen, Novel

Murine Model of Chronic Granulomatous Lung Inflammation Elicited by Carbon Nanotubes. Am.J Respir.Cell Mol.Biol 45 (2011) 858-866.

[59] I. Huizar, A. Malur, J. Patel, M. McPeek, L. Dobbs, C. Wingard, B.P. Barna, M.J. Thomassen, The role of PPARgamma in carbon nanotube-elicited granulomatous lung inflammation. Respir.Res. 14 (2013) 7.

[60] S. Hussain, S. Sangtian, S.M. Anderson, R.J. Snyder, J.D. Marshburn, A.B. Rice, J.C. Bonner, S. Garantziotis, Inflammasome activation in airway epithelial cells after multi-walled carbon nanotube exposure mediates a profibrotic response in lung fibroblasts. Part Fibre.Toxicol. 11 (2014) 28.

[61] T. Hussell, T.J. Bell, Alveolar macrophages: plasticity in a tissue-specific context. Nat.Rev.Immunol. 14 (2014) 81-93.

[62] M.C. Iannuzzi, J.R. Fontana, Sarcoidosis: clinical presentation, immunopathogenesis, and therapeutics. JAMA 305 (2011) 391-399.

[63] K. Iio, T.U. Iio, Y. Okui, H. Ichikawa, Y. Tanimoto, N. Miyahara, A. Kanehiro, M. Tanimoto, Y. Nakata, M. Kataoka, Experimental pulmonary granuloma mimicking sarcoidosis induced by Propionibacterium acnes in mice. Acta Med.Okayama 64 (2010) 75-83.

[64] T. Ito, J.M. Connett, S.L. Kunkel, A. Matsukawa, The linkage of innate and adaptive immune response during granulomatous development. Frontiers in Immunology 4 (2013).

[65] G. Izbicki, R. Chavko, G.I. Banauch, M.D. Weiden, K.I. Berger, T.K. Aldrich, C. Hall, K.J. Kelly, D.J. Prezant, World Trade Center "Sarcoid-Like" Granulomatous Pulmonary Disease in New York City Fire Department Rescue Workers. Chest 131 (2007) 1414-1423.

[66] M.K. Jain, P.M. Ridker, Anti-inflammatory effects of statins: clinical evidence and basic mechanisms. Nat.Rev.Drug Discov. 4 (2005) 977-987.

[67] D.K. Kajdasz, M.A. Judson, L.C. Mohr, Jr., D.T. Lackland, Geographic variation in sarcoidosis in South Carolina: its relation to socioeconomic status and health care indicators. Am J Epidemiol. 150 (1999) 271-278.

[68] D.K. Kajdasz, D.T. Lackland, L.C. Mohr, M.A. Judson, A current assessment of rurally linked exposures as potential risk factors for sarcoidosis. Ann.Epidemiol. 11 (2001) 111-117.

[69] T. Kawasaki, T. Kawai, Toll-like receptor signaling pathways. Front Immunol. 5 (2014) 461.

[70] M.A. Kennedy, G.C. Barrera, K. Nakamura, A. Baldan, P. Tarr, M.C. Fishbein, J. Frank, O.L. Francone, P.A. Edwards, ABCG1 has a critical role in mediating

cholesterol efflux to HDL and preventing cellular lipid accumulation. Cell Metabolism 1 (2005) 121-131.

[71] D. Kielar, W. Dietmaier, T. Langmann, C. Aslanidis, M. Probst, M. Naruszewicz, G. Schmitz, Rapid quantification of human ABCA1 mRNA in various cell types and tissues by real-time reverse transcription-PCR. Clin.Chem. 47 (2001) 2089-2097.

[72] G. Kirkil, E.E. Lower, R.P. Baughman, Predictors of Mortality in Pulmonary Sarcoidosis. Chest 153 (2018) 105-113.

[73] M. Kobayashi, M.J. Thomassen, T. Rambasek, T.L. Bonfield, B. Raychaudhuri, A. Malur, A.R. Winkler, B.P. Barna, S.J. Goldman, M.S. Kavuru, An inverse relationship between peroxisome proliferator-activated receptor gamma and allergic airway inflammation in an allergen challenge model. Ann.Allergy Asthma Immunol 95 (2005) 468-473.

[74] M. Koseki, K. Hirano, D. Masuda, C. Ikegami, M. Tanaka, A. Ota, J.C. Sandoval, Y. Nakagawa-Toyama, S.B. Sato, T. Kobayashi, Y. Shimada, Y. Ohno-Iwashita, F. Matsuura, I. Shimomura, S. Yamashita, Increased lipid rafts and accelerated lipopolysaccharide-induced tumor necrosis factor-alpha secretion in Abca1-deficient macrophages. J.Lipid Res. 48 (2007) 299-306.

[75] M.E. Kreider, J.D. Christie, B. Thompson, L. Newman, C. Rose, J. Barnard, E. Bresnitz, M.A. Judson, D.T. Lackland, M.D. Rossman, Relationship of environmental exposures to the clinical phenotype of sarcoidosis. Chest 128 (2005) 207-215.

[76] S. Kunkel, N.W. Lukacs, R.M. Strieter, S.W. Chensue, Animal models of granulomatous inflammation. Semin.Respir.Infect. 13 (1998) 221-228.

[77] A. Kveim, En ny og spesifikk kutan-reaksjon ved Boecks sarcoid. Nord Med 9 (1941) 169-172.

[78] C.W. Lam, J.T. James, R. McCluskey, S. Arepalli, R.L. Hunter, A review of carbon nanotube toxicity and assessment of potential occupational and environmental health risks. Crit Rev.Toxicol. 36 (2006) 189-217.

[79] C.W. Lam, J.T. James, R. McCluskey, R.L. Hunter, Pulmonary toxicity of single-wall carbon nanotubes in mice 7 and 90 days after intratracheal instillation. Toxicol.Sci 77 (2004) 126-134.

[80] P. Linsel-Nitschke, A.R. Tall, HDL as a target in the treatment of atherosclerotic cardiovascular disease. Nat.Rev.Drug Discov. 4 (2005) 193-205.

[81] M.F. Lipscomb, C.R. Lyons, G. Nunez, E.J. Ball, P. Stastny, W. Vial, V. Lem, J. Weissler, L.M. Miller, Human alveolar macrophages: HLA-DR-positive

macrophages that are poor stimulators of a primary mixed leukocyte reaction. J.Immunol. 136 (1986) 497-504.

[82] K.J. Livak, T.D. Schmittgen, Analysis of relative gene expression data using real-time quantitative PCR and the 2(-Delta Delta C(T)) Method. Methods 25 (2001) 402-408.

[83] B. Lu, B.J. Rutledge, L. Gu, J. Fiorillo, N.W. Lukacs, S.L. Kunkel, R. North, C. Gerard, B.J. Rollins, Abnormalities in monocyte recruitment and cytokine expression in monocyte chemoattractant protein 1-deficient mice. J.Exp.Med. 187 (1998) 601-608.

[84] J.P. Lynch, III, Y.L. Ma, M.N. Koss, E.S. White, Pulmonary sarcoidosis. Semin.Respir.Crit Care Med. 28 (2007) 53-74.

[85] C.R. Lyons, E.J. Ball, G.B. Toews, J.C. Weissler, P. Stastny, M.F. Lipscomb, Inability of human alveolar macrophages to stimulate resting T cells correlates with decreased antigen-specific T cell-macrophage binding. J.Immunol. 137 (1986) 1173-1180.

[86] A. Malur, B.P. Barna, J. Patel, M. McPeek, C.J. Wingard, L. Dobbs, M.J. Thomassen, Exposure to a Mycobacterial Antigen, ESAT-6, Exacerbates Granulomatous and Fibrotic Changes in a Multiwall Carbon Nanotube Model of Chronic Pulmonary Disease. J Nanomed Nanotechnol 6 (2015) 340.

[87] A. Malur, I. Huizar, G. Wells, B.P. Barna, A.G. Malur, M.J. Thomassen, Lentivirus-ABCG1 instillation reduces lipid accumulation and improves lung compliance in GM-CSF knock-out mice. Biochem.Biophys.Res.Commun. 415 (2011) 288-293.

[88] A. Malur, A.J. Mccoy, S. Arce, B.P. Barna, M.S. Kavuru, A.G. Malur, M.J. Thomassen, Deletion of PPARg in alveolar macrophages is associated with a Th-1 pulmonary inflammatory response. J.Immunol. 182 (2009) 5816-5822.

[89] T. Martin, P.M. Cardarelli, G.C. Parry, K.A. Felts, R.R. Cobb, Cytokine induction of monocyte chemoattractant protein-1 gene expression in human endothelial cells depends on the cooperative action of NF-kappa B and AP-1. Eur.J.Immunol. 27 (1997) 1091-1097.

[90] J. McNeish, R.J. Aiello, D. Guyot, T. Turi, C. Gabel, C. Aldinger, K.L. Hoppe, M.L. Roach, L.J. Royer, J. de Wet, C. Broccardo, G. Chimini, O.L. Francone, High density lipoprotein deficiency and foam cell accumulation in mice with targeted disruption of ATP-binding cassette transporter-1. Proc.Natl.Acad.Sci.U.S.A 97 (2000) 4245-4250.

[91] M. McPeek, A. Malur, D.A. Tokarz, G. Murray, B.P. Barna, M.J. Thomassen, PPAR-gamma pathways attenuate pulmonary granuloma formation in a carbon

nanotube induced murine model of sarcoidosis. Biochem.Biophys.Res.Commun.2018).

[92] A. Miller, Sarcoidosis, firefighters sarcoidosis, and World Trade Center "sarcoid-like" granulomatous pulmonary disease. Chest 132 (2007) 2053.

[93] N. Milman, G. Lisby, S. Friis, L. Kemp, Prolonged culture for mycobacteria in mediastinal lymph nodes from patients with pulmonary sarcoidosis. A negative study. Sarcoidosis.Vasc.Diffuse.Lung Dis. 21 (2004) 25-28.

[94] M. Mirsaeidi, R.F. Machado, D. Schraufnagel, N.J. Sweiss, R.P. Baughman, RAcial difference in sarcoidosis mortality in the united states. Chest 147 (2015) 438-449.

[95] A. Mohan, A. Malur, M. McPeek, B.P. Barna, L.M. Schnapp, M.J. Thomassen, S.A. Gharib, Transcriptional survey of alveolar macrophages in a murine model of chronic granulomatous inflammation reveals common themes with human sarcoidosis. Am.J.Physiol Lung Cell Mol.Physiol 314 (2018) L617-L625.

[96] J. Muller, F. Huaux, N. Moreau, P. Misson, J.F. Heilier, M. Delos, M. Arras, A. Fonseca, J.B. Nagy, D. Lison, Respiratory toxicity of multi-wall carbon nanotubes. Toxicol.Appl.Pharmacol. 207 (2005) 221-231.

[97] J. Muller-Quernheim, M. Schurmann, S. Hofmann, K.I. Gaede, A. Fischer, A. Prasse, G. Zissel, S. Schreiber, Genetics of sarcoidosis. Clin.Chest Med 29 (2008) 391-414, viii.

[98] L.E. Murr, K.F. Soto, K.M. Garza, P.A. Guerrero, F. Martinez, E.V. Esquivel, D.A. Ramirez, Y. Shi, J.J. Bang, J. Venzor, III, Combustion-generated nanoparticulates in the El Paso, TX, USA / Juarez, Mexico Metroplex: their comparative characterization and potential for adverse health effects. Int.J.Environ.Res.Public Health 3 (2006) 48-66.

[99] C. Nathan, Metchnikoff's Legacy in 2008. Nat Immunol 9 (2008) 695-698.

[100] B.M. Necela, W. Su, E.A. Thompson, Toll-like receptor 4 mediates cross-talk between peroxisome proliferator-activated receptor gamma and nuclear factor-kappaB in macrophages. Immunology 125 (2008) 344-358.

[101] L.S. Newman, C.S. Rose, E.A. Bresnitz, M.D. Rossman, J. Barnard, M. Frederick, M.L. Terrin, S.E. Weinberger, D.R. Moller, G. McLennan, G. Hunninghake, L. DePalo, R.P. Baughman, M.C. Iannuzzi, M.A. Judson, G.L. Knatterud, B.W. Thompson, A.S. Teirstein, H. Yeager, Jr., C.J. Johns, D.L. Rabin, B.A. Rybicki, R. Cherniack, A case control etiologic study of sarcoidosis: environmental and occupational risk factors. Am.J Respir Crit Care Med 170 (2004) 1324-1330.

[102] A.S. Nishikaku, R.F. Molina, L.C. Ribeiro, R. Scavone, B.P. Albe, C.S. Cunha, E. Burger, Nitric oxide participation in granulomatous response induced by Paracoccidioides brasiliensis infection in mice. Med Microbiol.Immunol. 198 (2009) 123-135.

[103] A.W. O'Regan, G.L. Chupp, J.A. Lowry, M. Goetschkes, N. Mulligan, J.S. Berman, Osteopontin is associated with T cells in sacroid granulomas and has T cell adhesive and cytokin-like properties in vitro. J.Immunol. 162 (1999) 1024-1031.

[104] A.W. O'Regan, J.M. Hayden, S. Body, L. Liaw, N. Mulligan, M. Goetschkes, J.S. Berman, Abnormal pulmonary granuloma formation in osteopontin-deficient mice. Am.J.Respir.Crit.Care Med. 164 (2001) 2243-2247.

[105] K.A. Oswald-Richter, D.C. Beachboard, E.H. Seeley, S. Abraham, B.E. Shepherd, C.A. Jenkins, D.A. Culver, R.M. Caprioli, W.P. Drake, Dual analysis for mycobacteria and propionibacteria in sarcoidosis BAL. J.Clin.Immunol. 32 (2012) 1129-1140.

[106] R. Out, W. Jessup, G.W. Le, M. Hoekstra, I.C. Gelissen, Y. Zhao, L. Kritharides, G. Chimini, J. Kuiper, M.J. Chapman, T. Huby, T.J. Van Berkel, E.M. Van, Coexistence of foam cells and hypocholesterolemia in mice lacking the ABC transporters A1 and G1. Circ.Res. 102 (2008) 113-120.

[107] A.J. Pagan, L. Ramakrishnan, The Formation and Function of Granulomas. Annu.Rev.Immunol. 36 (2018) 639-665.

[108] V. Palchevskiy, N. Hashemi, S.S. Weigt, Y.Y. Xue, A. Derhovanessian, M.P. Keane, R.M. Strieter, M.C. Fishbein, J.C. Deng, J.P. Lynch, III, R. Elashoff, J.A. Belperio, Immune response CC chemokines CCL2 and CCL5 are associated with pulmonary sarcoidosis. Fibrogenesis.Tissue Repair 4 (2011) 10.

[109] M. Pennings, I. Meurs, D. Ye, R. Out, M. Hoekstra, T.J. Van Berkel, E.M. Van, Regulation of cholesterol homeostasis in macrophages and consequences for atherosclerotic lesion development. FEBS Lett. 580 (2006) 5588-5596.

[110] A. Pietinalho, M. Ohmichi, M. Hirasawa, Y. Hiraga, A.B. Lofroos, O. Selroos, Familial sarcoidosis in Finland and Hokkaido, Japan--a comparative study. Respir.Med. 93 (1999) 408-412.

[111] A. Pietinalho, M. Ohmichi, M. Hirasawa, Y. Hiraga, A.B. Lofroos, O. Selroos, Familial sarcoidosis in Finland and Hokkaido, Japan--a comparative study. Respir.Med. 93 (1999) 408-412.

[112] D.W. Porter, A.F. Hubbs, R.R. Mercer, N. Wu, M.G. Wolfarth, K. Sriram, S. Leonard, L. Battelli, D. Schwegler-Berry, S. Friend, M. Andrew, B.T. Chen, S. Tsuruoka, M. Endo, V. Castranova, Mouse pulmonary dose- and time course-

responses induced by exposure to multi-walled carbon nanotubes. Toxicology 269 (2010) 136-147.

[113] A. Prasse, P. Engelhard, L. Plappert, V. Hornung, F. Bauernfeind, B. J+ñger, The NLRP3 Inflammasome and IL-1+¦ Pathway Have a Pivotal Role in Granuloma Formation of Sarcoidosis, C21. ALVEOLAR MACROPHAGE DIVERSITY IN LUNG INJURY AND REPAIR, American Thoracic Society, 2018, pp. A4492.

[114] D.J. Prezant, A. Dhala, A. Goldstein, D. Janus, F. Ortiz, T.K. Aldrich, K.J. Kelly, The incidence, prevalence, and severity of sarcoidosis in New York City firefighters. Chest 116 (1999) 1183-1193.

[115] M. Ricote, C.K. Glass, PPARs and molecular mechanisms of transrepression. Biochim.Biophys.Acta 1771 (2007) 926-935.

[116] M. Ricote, A.C. Li, T.M. Willson, C.J. Kelly, C.K. Glass, The peroxisome proliferator-activated receptor-g is a negative regulator of macrophage activation. Nature 391 (1998) 79-82.

[117] M. Ricote, J.S. Welch, C.K. Glass, Regulation of macrophage gene expression by the peroxisome proliferator-activated receptor-gamma. Horm.Res. 54 (2000) 275-280.

[118] F. Romero, D. Shah, M. Duong, R.B. Penn, M.B. Fessler, J. Madenspacher, W. Stafstrom, M. Kavuru, B. Lu, C.B. Kallen, K. Walsh, R. Summer, A pneumocyte-macrophage paracrine lipid axis drives the lung toward fibrosis. Am.J.Respir.Cell Mol.Biol. 53 (2015) 74-86.

[119] M.D. Rossman, B. Thompson, M. Frederick, M. Maliarik, M.C. Iannuzzi, B.A. Rybicki, J.P. Pandey, L.S. Newman, E. Magira, B. Beznik-Cizman, D. Monos, HLA-DRB1*1101: a significant risk factor for sarcoidosis in blacks and whites. Am.J.Hum.Genet. 73 (2003) 720-735.

[120] B.A. Rybicki, M. Major, J.J. Popovich, M. Maliarik, M.C. Iannuzzi, Racial differences in sarcoidosis incidence: a five year study in a health maintenance organization. Am.J.Epidemiol. 145 (1997) 234-241.

[121] J. Schnerch, A. Prasse, D. Vlachakis, K.L. Schuchardt, D.V. Pechkovsky, T. Goldmann, K.I. Gaede, J. Muller-Quernheim, G. Zissel, Functional Toll-Like Receptor 9 Expression and CXCR3 Ligand Release in Pulmonary Sarcoidosis. Am.J.Respir.Cell Mol.Biol. 55 (2016) 749-757.

[122] M. Schurmann, R. Kwiatkowski, M. Albrecht, A. Fischer, J. Hampe, J. Muller-Quernheim, E. Schwinger, S. Schreiber, Study of Toll-like receptor gene loci in sarcoidosis. Clin.Exp.Immunol. 152 (2008) 423-431.

[123] M. Schurmann, P. Reichel, B. Muller-Myhsok, M. Schlaak, J. Muller-Quernheim, E. Schwinger, Results from a genome-wide search for predisposing genes in sarcoidosis. Am.J.Respir.Crit.Care Med. 164 (2001) 840-846.

[124] L.E. Siltzbach, The Kveim test in sarcoidosis. A study of 750 patients. JAMA 178 (1961) 476-482.

[125] R.J. Snelgrove, A. Godlee, T. Hussell, Airway immune homeostasis and implications for influenza-induced inflammation. Trends Immunol. 32 (2011) 328-334.

[126] M.B. Snipes, Long-term retention and clearance of particles inhaled by mammalian species. Crit Rev.Toxicol. 20 (1989) 175-211.

[127] G. Song, D.B. Darr, C.M. Santos, M. Ross, A. Valdivia, J.L. Jordan, B.R. Midkiff, S. Cohen, N. Nikolaishvili-Feinberg, C.R. Miller, T.K. Tarrant, A.B. Rogers, A.C. Dudley, C.M. Perou, W.C. Zamboni, Effects of tumor microenvironment heterogeneity on nanoparticle disposition and efficacy in breast cancer tumor models. Clin.Cancer Res. 20 (2014) 6083-6095.

[128] N.J. Sweiss, E.E. Lower, M. Mirsaeidi, S. Dudek, J.G. Garcia, D. Perkins, P.W. Finn, R.P. Baughman, Rituximab in the treatment of refractory pulmonary sarcoidosis. Eur.Respir.J. 43 (2014) 1525-1528.

[129] J.J. Swigris, A.L. Olson, T.J. Huie, E.R. Fernandez-Perez, J. Solomon, D. Sprunger, K.K. Brown, Sarcoidosis-related mortality in the United States from 1988 to 2007. Am.J.Respir.Crit Care Med. 183 (2011) 1524-1530.

[130] A.C. Thomas, W.J. Eijgelaar, M.J. Daemen, A.C. Newby, Foam Cell Formation In Vivo Converts Macrophages to a Pro-Fibrotic Phenotype. PLoS.One. 10 (2015) e0128163.

[131] M.J. Thomassen, B.P. Barna, A. Malur, T.L. Bonfield, C.F. Farver, A. Malur, H. Dalrymple, M.S. Kavuru, M. Febbraio, ABCG1 is deficient in alveolar macrophages of GM-CSF knock-out mice and patients with pulmonary alveolar proteinsosis. J.Lipid Res. 48 (2007) 2762-2768.

[132] P. Tontonoz, B.M. Spiegelman, Fat and Beyond: The Diverse Biology of PPARgamma. Annual Review of Biochemistry 77 (2008) 289-312.

[133] W. Van den Broeck, A. Derore, P. Simoens, Anatomy and nomenclature of murine lymph nodes: Descriptive study and nomenclatory standardization in BALB/cAnNCrl mice. J.Immunol.Methods 312 (2006) 12-19.

[134] A.M. Vaughan, J.F. Oram, ABCA1 and ABCG1 or ABCG4 act sequentially to remove cellular cholesterol and generate cholesterol-rich HDL. J.Lipid Res. 47 (2006) 2433-2443.

[135] N. Wang, D. Lan, W. Chen, F. Matsuura, A.R. Tall, ATP-binding cassette transporters G1 and G4 mediate cellular cholesterol efflux to high-density lipoproteins. Proc Natl.Acad.Sci.U.S.A 101 (2004) 9774-9779.

[136] X. Wang, H.L. Collins, M. Ranalletta, I.V. Fuki, J.T. Billheimer, G.H. Rothblat, A.R. Tall, D.J. Rader, Macrophage ABCA1 and ABCG1, but not SR-BI, promote macrophage reverse cholesterol transport in vivo. J Clin Invest 117 (2007) 2216-2224.

[137] T.E. Wessendorf, F. Bonella, U. Costabel, Diagnosis of Sarcoidosis. Clin.Rev.Allergy Immunol. 49 (2015) 54-62.

[138] M. Westerterp, E.L. Gautier, A. Ganda, M.M. Molusky, W. Wang, P. Fotakis, N. Wang, G.J. Randolph, V.D. D'Agati, L. Yvan-Charvet, A.R. Tall, Cholesterol Accumulation in Dendritic Cells Links the Inflammasome to Acquired Immunity. Cell Metab 25 (2017) 1294-1304.

[139] M. Westerterp, A.J. Murphy, M. Wang, T.A. Pagler, Y. Vengrenyuk, M.S. Kappus, D.J. Gorman, P.R. Nagareddy, X. Zhu, S. Abramowicz, J.S. Parks, C. Welch, E.A. Fisher, N. Wang, L. Yvan-Charvet, A.R. Tall, Deficiency of ATP-binding cassette transporters A1 and G1 in macrophages increases inflammation and accelerates atherosclerosis in mice. Circ.Res. 112 (2013) 1456-1465.

[140] J.A. Whitsett, S.E. Wert, T.E. Weaver, Alveolar surfactant homeostasis and the pathogenesis of pulmonary disease. Annu.Rev.Med 61 (2010) 105-119.

[141] J.A. Whitsett, S.E. Wert, T.E. Weaver, Diseases of pulmonary surfactant homeostasis. Annu.Rev.Pathol. 10 (2015) 371-393.

[142] R.H. Winterbauer, J. Lammert, M. Selland, R. Wu, D. Corley, S.C. Springmeyer, Bronchoalveolar lavage cell populations in the diagnosis of sarcoidosis. Chest 104 (1993) 352-361.

[143] A.J. Wojcik, M.D. Skaflen, S. Srinivasan, C.C. Hedrick, A critical role for ABCG1 in macrophage inflammation and lung homeostasis. J Immunol. 180 (2008) 4273-4282.

[144] M. Yarmolinsky, R. Hoess, The Legacy of Nat Sternberg: The Genesis of Cre-lox Technology. Annu.Rev.Virol. 2 (2015) 25-40.

[145] K. Yasuda, A. Sato, K. Nishimura, K. Chida, H. Hayakawa, Phospholipid analysis of alveolar macrophages and bronchoalveolar lavage fluid following bleomycin administration to rabbits. Lung 172 (1994) 91-102.

[146] L. Yvan-Charvet, M. Ranalletta, N. Wang, S. Han, N. Terasaka, R. Li, C. Welch, A.R. Tall, Combined deficiency of ABCA1 and ABCG1 promotes foam cell accumulation and accelerates atherosclerosis in mice. J Clin Invest 117 (2007) 3900-3908.

[147] L. Yvan-Charvet, C. Welch, T.A. Pagler, M. Ranalletta, M. Lamkanfi, S. Han, M. Ishibashi, R. Li, N. Wang, A.R. Tall, Increased Inflammatory Gene Expression in ABC Transporter-Deficient Macrophages: Free Cholesterol Accumulation, Increased Signaling via Toll-Like Receptors, and Neutrophil Infiltration of Atherosclerotic Lesions. Circulation 118 (2008) 1837-1847.

[148] W. Zhao, L. Wang, M. Zhang, P. Wang, L. Zhang, C. Yuan, J. Qi, Y. Qiao, P.C. Kuo, C. Gao, NF-kappaB- and AP-1-mediated DNA looping regulates osteopontin transcription in endotoxin-stimulated murine macrophages. J.Immunol. 186 (2011) 3173-3179.

APPENDIX A

East Carolina University

ıimal Care and
Use Commitee
212 Ed Warren Life
Sciences Building
East Carolina University
Greenville, NC 27834

252-744-2436 office
252-744-2355 fax

October 28, 2016

Mary Jane Thomassen, Ph.D.
Department of Medicine
Brody 3E-115, MS# 628
ECU Brody School of Medicine

Dear Drs. Thomassen:

The Amendment to your Animal Use Protocol entitled, "Carbon Nanotubes as a Tool for Generating an Experimental Model of Pulmonary Sarcoidosis" (AUP #J199b) was reviewed by this institution's Animal Care and Use Committee on October 28, 2016. The following action was taken by the Committee:

"Approved as submitted"

Please contact Aaron Hinkle at 744-2997 prior to hazard use

A copy is enclosed for your laboratory files. Please be reminded that all animal procedures must be conducted as described in the approved Animal Use Protocol. Modifications of these procedures cannot be performed without prior approval of the ACUC. The Animal Welfare Act and Public Health Service Guidelines require the ACUC to suspend activities not in accordance with approved procedures and report such activities to the responsible University Official (Vice Chancellor for Health Sciences or Vice Chancellor for Academic Affairs) and appropriate federal Agencies. **Please ensure that all personnel associated with this protocol have access to this approved copy of the AUP and are familiar with its contents.**

Sincerely yours,

Susan McRae, Ph.D.
Chair, Animal Care and Use Committee

SM/jd

Enclosure